

State Emergency Service of Ukraine  
National Academy of Sciences of Ukraine  
Ukrainian Hydrometeorological Institute of SES of Ukraine and NAS of Ukraine

# Assessment Report

## Consequences of the full-scale Russian invasion for air quality in Ukraine

24.02.2022 – 24.02.2026

2026



The research conducted by the staff of the Laboratory of Atmospheric Air Monitoring, Department of Atmosphere Monitoring, Ukrainian Hydrometeorological Institute of the State Emergency Service of Ukraine and the National Academy of Sciences of Ukraine

Authors:

Mykhailo SAVENETS, PhD, Head of Department of Atmosphere Monitoring

Liudmyla NADTOCHII, PhD, senior researcher

Tetiana KOZLENKO, researcher

Kateryna KOMISAR, lead engineer

Antonina UMANETS, lead engineer

Daria HRAMA, engineer

Natalia ZHEMERA, engineer

Sofia KRAINYK, engineer

Maryna RUDAS, engineer

The assessment report is a synthesis of scientific research conducted within the framework of a number of research projects and studies:

- №9/21 «Current tendencies in spatio-temporal distribution of atmospheric chemical compounds based on the integration of data measurements» (2021–2023) supported by the SES of Ukraine
- «Development of the multitasking geoportal of environmental monitoring and forecast» (2021–2025) according to the plan of the NAS of Ukraine for 2021-2025.
- «Development of the system for atmospheric air pollution operational monitoring over Ukrainian cities using satellite data» (2021–2023) within the framework of the targeted research program “Aerospace Observations of the Environment for Sustainable Development and Security” for 2021-2023.
- №2022.01/0121 «Geoinformation system for spatial assessment of environmental degradation in Ukraine due to Russian aggression» (2023-2024) supported by the National Research Foundation of Ukraine withing the the Call “Science for the Reconstruction of Ukraine in Wartime and Post-War Periods”.
- «Investigation of Aerosol Pollution Characteristics in the Atmospheric Air During Armed Conflicts in Ukraine» (2024). Additional departmental research topic for 2024 led by young scientists of the National Academy of Sciences of Ukraine, within the framework of targeted financial support for young researchers who presented scientific reports at the meetings of the Presidium of the NAS of Ukraine in 2023.
- №8/24 «Development of Software and Modeling Tools for Assessing the State of Atmospheric Air Pollution over the Territory of Ukraine» (2024-2026 pp.) supported by the SES of Ukraine
- №2025.05/0005 «Development of a Methodology for the Application of Seamless Numerical Models to Assess the Impact of Armed Conflicts on Atmospheric Air Quality» (2026) supported by the National Research Foundation of Ukraine As within the Call for Presidential Grants of Ukraine supporting research and development by young scientists with a PhD (Candidate of Sciences) degree.

Photo and illustrations in pages 1, 8, 14, 17, 23, 45 were taken from the Pixabay (<https://pixabay.com/>), that are distributed by the CC0 license (instrument).

Maps and plots were produced by the staff of the Laboratory of Atmospheric Air Monitoring, Ukrainian Hydrometeorological Institute of the State Emergency Service of Ukraine and the National Academy of Sciences of Ukraine

The report materials may be freely used and distributed, provided that a reference to the report is clearly indicated.

Contact person: Mykhailo Savenets, [savenets@uhmi.org.ua](mailto:savenets@uhmi.org.ua)

## INTRODUCTION

This assessment report presents research and analysis of the impacts of four years of the full-scale Russian invasion (24.02.2022–24.02.2026) on air quality in Ukraine, based on satellite remote sensing data and ground-based monitoring stations of the hydrometeorological observation network.

The assessment report includes an executive summary for governmental authorities and policymakers, as well as an extended analysis of both short-term impacts and long-term effects of military activities on atmospheric pollution. The analysis of pollutant concentrations is preceded by an examination of changes in prevailing meteorological conditions and the distribution of landscape fires, in order to account for their contribution to atmospheric pollution formation. The report concludes with findings summarizing the main impacts of the full-scale Russian invasion on air quality, along with recommendations for optimizing the integrated use of different sources of air pollution data and for incorporating the identified changes into decision-making processes. All methodological and technical aspects of the conducted research are presented in a dedicated section following the conclusions and recommendations.

## EXECUTIVE SUMMARY FOR GOVERNMENT AUTHORITIES AND POLICYMAKERS

Over the four years (24.02.2022–24.02.2026) of the full-scale Russian invasion, Ukraine has experienced an unprecedented impact on economic, social, and environmental processes in modern history. Thousands of missile and drone strikes, destruction of industrial facilities, devastation of cities, population displacement, and landscape fires caused by shelling – all these and many other processes have had a direct impact on air quality. Air quality is an important, though not always obvious, factor determining risks to human health and ecosystem functioning.

Assessing the impact of war on air quality is significantly more complex than traditional air pollution analysis under peacetime conditions, as it requires accounting for the simultaneous influence of multiple interacting factors. Ground-based monitoring networks effectively capture local changes in pollution levels but are unable to cover all areas affected by hostilities. An additional challenge is the loss of part of the monitoring network, particularly in areas closer to the front line. Satellite remote sensing of pollutants provides broad spatial coverage but has limited sensitivity to certain concentration changes and is dependent on cloud conditions. Moreover, due to the high variability of the atmosphere, where many pollutants rapidly disperse, deposit, or undergo chemical transformation, the temporal gap between emission and observation often complicates reliable impact assessment.

The analysis is further complicated by changes in the spatial distribution of landscape fires and the simultaneous action of multiple, often opposing, factors. On the one hand, missile strikes can cause strong short-term emissions of pollutants; on the other hand, the shutdown of industrial facilities leads to a reduction in regular emissions. Power outages increase the use of generators, while population displacement may reduce transport-related emissions in certain cities, although new war-related pollution sources emerge in these areas.

The most typical and widespread consequence of the war is the increased occurrence of episodes of high pollution levels following missile and drone attacks. On average, after each missile or drone strike, near-surface pollutant concentrations increase by 100–300% relative to pre-event levels, and in some extreme cases by more than 1000%. At the same time, the frequency of such events being captured by ground-based monitoring systems is low. This is due to the rapid dispersion of pollutants and the point-based nature of measurements at stationary monitoring stations.

Due to the use of only polar-orbiting satellites for air quality monitoring over Europe during 2022–2026, providing only one observation per day, most short-term high-pollution events following missile and drone attacks were not captured due to the temporal mismatch between emissions and satellite overpasses. In cases where the effects of

strong short-term emissions were observed, pollutant concentrations increased on average by 50–150% relative to typical values. At the same time, satellite methods enabled the detection of pollution associated with landscape fires, particularly those occurring along the front line as a result of shelling. For remote areas lacking ground-based monitoring, satellite remote sensing remains the only source of information on air quality.

Four years of full-scale war have affected overall air quality in the form of long-term effects. First and foremost, the consequences of the destruction of industrial facilities and cities are observed. According to satellite observations at the regional scale, a decrease in average pollution levels in industrial regions compared to the 2019–2021 period has been recorded, ranging from 8 to 30% depending on the pollutant. At the same time, ground-based observations from the hydrometeorological monitoring network, which better capture local changes, show more complex spatiotemporal dynamics. In front-line cities, increased pollution levels are observed due to intensified military activity. In large industrial cities, long-term trends mostly reflect a decrease in average pollution levels due to industrial destruction. In rear-area cities, mixed trends are observed, indicating a redistribution of pollutant concentrations.

It is important to emphasize the potentially misleading nature of observed pollution decreases in some industrial cities. Strong short-term emissions caused by missile strikes and resulting in industrial destruction may have a more severe impact on human health than long-term, regular, but controlled emissions from the operation of these facilities.

The war in Ukraine demonstrates that ground-based monitoring systems remain a key source of information on air pollution. The launch of the geostationary Sentinel-4 satellite in 2025 can significantly enhance monitoring capabilities. However, the combined observational data do not allow for a full reconstruction of air quality dynamics throughout the war. The most effective tool for this remains the application of numerical atmospheric modelling and chemical transport models.

## CONTENTS

List of abbreviations.....	7
Impact of meteorological conditions.....	8
Changes in the distribution of landscape fires.....	14
Changes in air quality	
Short-term impacts.....	17
Long-term effects.....	23
Conclusions.....	41
Recommendations.....	43
Research methodology.....	45
References.....	50

## LIST OF ABBREVIATIONS

### **Pollutants:**

CH<sub>2</sub>O – formaldehyde;  
C<sub>6</sub>H<sub>5</sub>OH – phenol;  
CO – carbon monoxide;  
H<sub>2</sub>S – hydrogen sulfide;  
HCl – hydrogen chloride;  
HF – hydrogen fluoride;  
NH<sub>3</sub> – ammonia;  
NO<sub>2</sub> – nitrogen dioxide;  
NO – nitrogen oxide;  
O<sub>3</sub> – ozone;  
SO<sub>2</sub> – sulfur dioxide;  
TSP – total suspended particles.

### **Systems, platforms:**

CDSE – Copernicus Data Space Ecosystem;  
FIRMS – Fire Information for Resource Management System.

### **Satellites and instruments:**

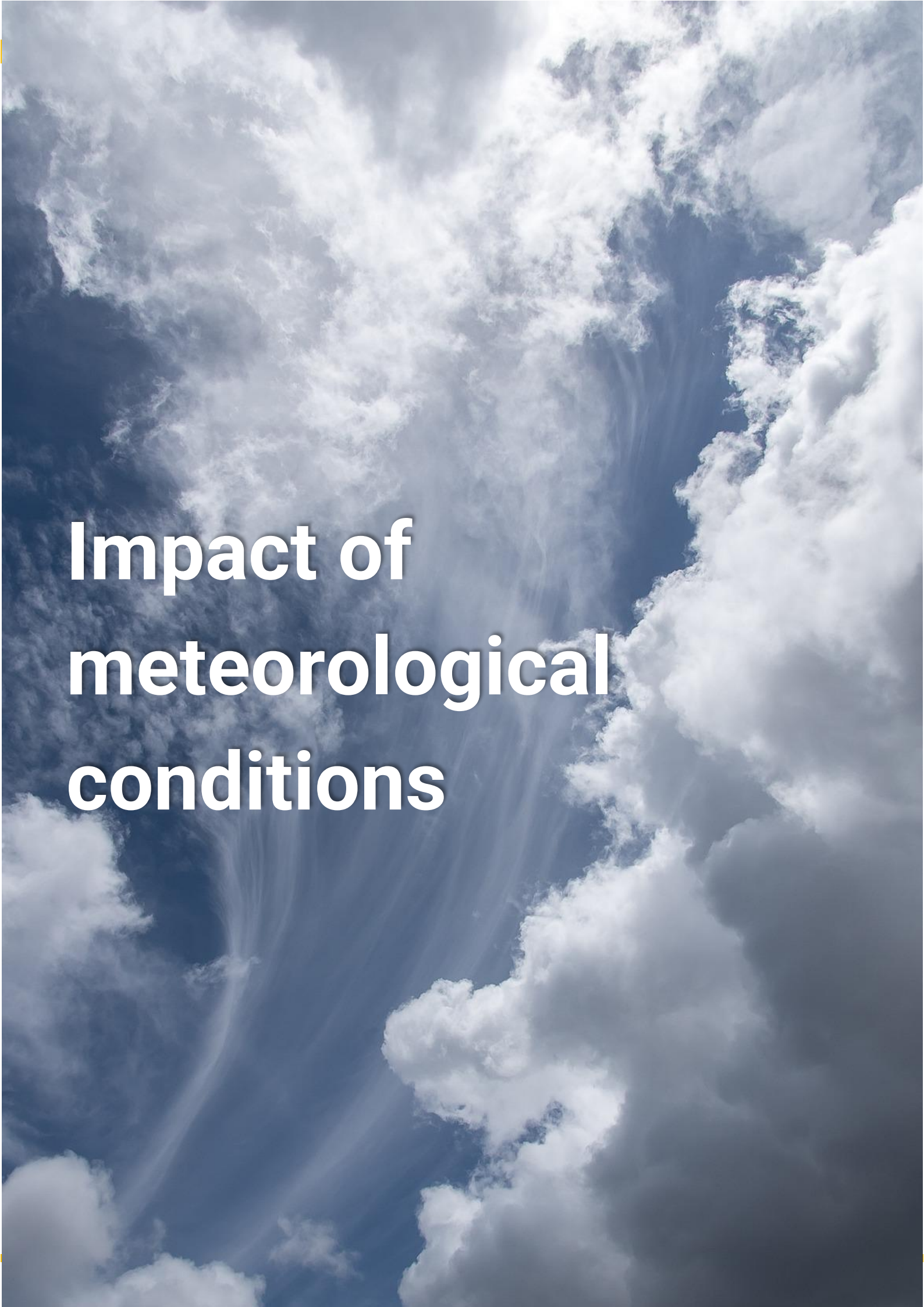
MODIS – Moderate Resolution Imaging Spectroradiometer;  
NOAA-20, -21 – National Oceanic and Atmospheric Administration -20, -21;  
Sentinel-5P – Sentinel-5 Precursor;  
Suomi NPP – Suomi National Polar-orbiting Partnership;  
TROPOMI – TROPospheric Monitoring Instrument;  
VIIRS – Visible Infrared Imaging Radiometer Suite.

### **Organizations and authorities:**

SES – State Emergency Service of Ukraine;  
NAS – National Academy of Sciences of Ukraine;  
UHMI – Ukrainian Hydrometeorological Institute of SES of Ukraine and NAS of Ukraine;  
CGO – Central Geophysical Observatory named after Boris Sreznevskiy.

### **Other:**

TPP – thermal power plant;  
CHP – combined heat and power plant;  
OFFL – offline Sentinel-5P data;  
VCD – vertical column density.



# **Impact of meteorological conditions**

After emissions of air pollutants enter the atmosphere, the formation of concentrations depends significantly on weather conditions<sup>1</sup>. Not all changes in air quality are associated with changes in emission volumes. Any analysis of atmospheric pollution should therefore be preceded by an examination of changes in key meteorological parameters that determine the deposition rate of pollutants, their dispersion conditions, and the rates of atmospheric chemical reactions leading to the transformation of some chemical species into others.

For example, a lower frequency of precipitation during a given season may lead to higher average concentrations of pollutants due to a significantly reduced rate of wet deposition<sup>2</sup>. Stronger winds promote better dispersion of pollutants, whereas a higher frequency of calm conditions contributes to the accumulation of pollutants in the near-surface atmospheric layer<sup>3</sup>. Temperature inversions (an increase in air temperature with height) promote the formation of atmospheric blocking layers, leading to air quality deterioration<sup>2</sup>. All these examples of prevailing weather impacts directly lead to changes in pollutant concentrations, which are not related to increases or decreases in emission levels.

Therefore, for a correct analysis of air quality changes caused by military activities, changes in meteorological parameters are analyzed first. Based on it, the degree of influence of prevailing weather conditions is determined.

In this report, the analysis of meteorological conditions focuses on four parameters:

- 1) near-surface **air temperature**, to account for atmospheric conditions affecting the chemical transformation of pollutants;
- 2) **total precipitation**, to account for the intensity of wet deposition;
- 3) **boundary layer height**, indicating the potential for vertical dispersion of pollutants;
- 4) near-surface **wind speed**, which determines the potential for horizontal dispersion of pollutants.

Near-surface **air temperature** during the period from spring 2022 to winter 2025/26 differed significantly from the values of the baseline period (2019–2021) used for comparison of air quality. [Fig. 1](#) shows seasonal changes in near-surface air temperature during the period of the full-scale Russian invasion.

The most pronounced changes in near-surface air temperature during 2022–2025/26 were observed in the transitional seasons. Each spring of this period was, on average, 1–4°C warmer than in the baseline period. For the spring season, higher air temperatures indicate a shift in meteorological conditions toward those more favorable for chemical transformation and a background decrease in concentrations of several pollutants (such as NO<sub>2</sub> and CO<sup>4,5</sup>), but enhanced formation of O<sub>3</sub> and CH<sub>2</sub>O<sup>6</sup>. In contrast, autumn near-surface air temperatures were significantly lower than in the baseline period, resulting in opposite effects compared to spring conditions.

Among the summer seasons, particular attention should be given to the hotter summer of 2024 and the general tendency toward higher temperatures in the southern regions. The last two winters were contrasting: the winter of 2024/25 was significantly warmer, while the winter of 2025/26 was colder compared to the baseline period of 2019–2021.

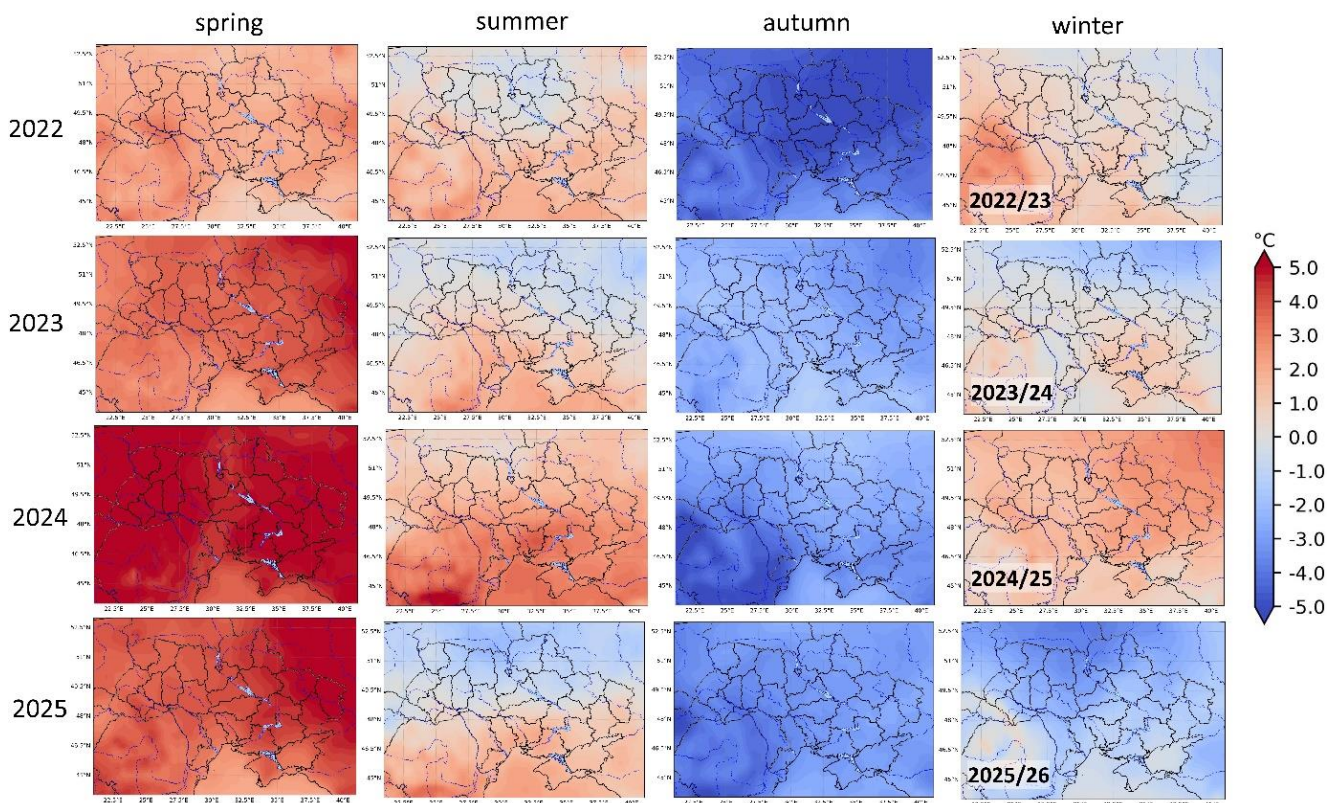


Fig. 1. Changes in the seasonal mean near-surface air temperature (°C) since the beginning of the full-scale invasion (spring 2022 – winter 2025/2026) compared to the mean temperature of the corresponding season during the baseline period (2019–2021)

Changes in **total precipitation** over the period from spring 2022 to winter 2025/26 across the territory of Ukraine were more heterogeneous compared to the baseline period (2019–2021). [Fig. 2](#) presents the seasonal changes in total precipitation during the period of the full-scale Russian invasion.

The most uniform feature is the increase in total precipitation during autumn seasons, particularly in 2022 and 2023. Given that precipitation is the primary removal mechanism for most atmospheric pollutants, autumn conditions were generally more favorable for reducing pollution levels. Of particular interest is the spatial distribution of summer precipitation. Throughout the entire period of the full-scale Russian invasion, an increase in precipitation was observed in northern Ukraine (and thus more favorable conditions for pollutant removal), whereas a precipitation deficit was recorded in the southern regions (i.e., conditions more conducive to pollutant accumulation). In 2024 and 2025, summer precipitation in southern Ukraine was 100–150 mm lower than during the 2019–2021 baseline period.

A decrease in the intensity of wet deposition was also observed in winter 2024/25 across the entire territory of Ukraine, in winter 2025/26 in the western regions, as well as in spring 2022 and 2024 over most of the country. In contrast, more favorable conditions for pollutant removal were recorded in spring 2023 in the southeastern regions and in winter 2023/24 across most of Ukraine.

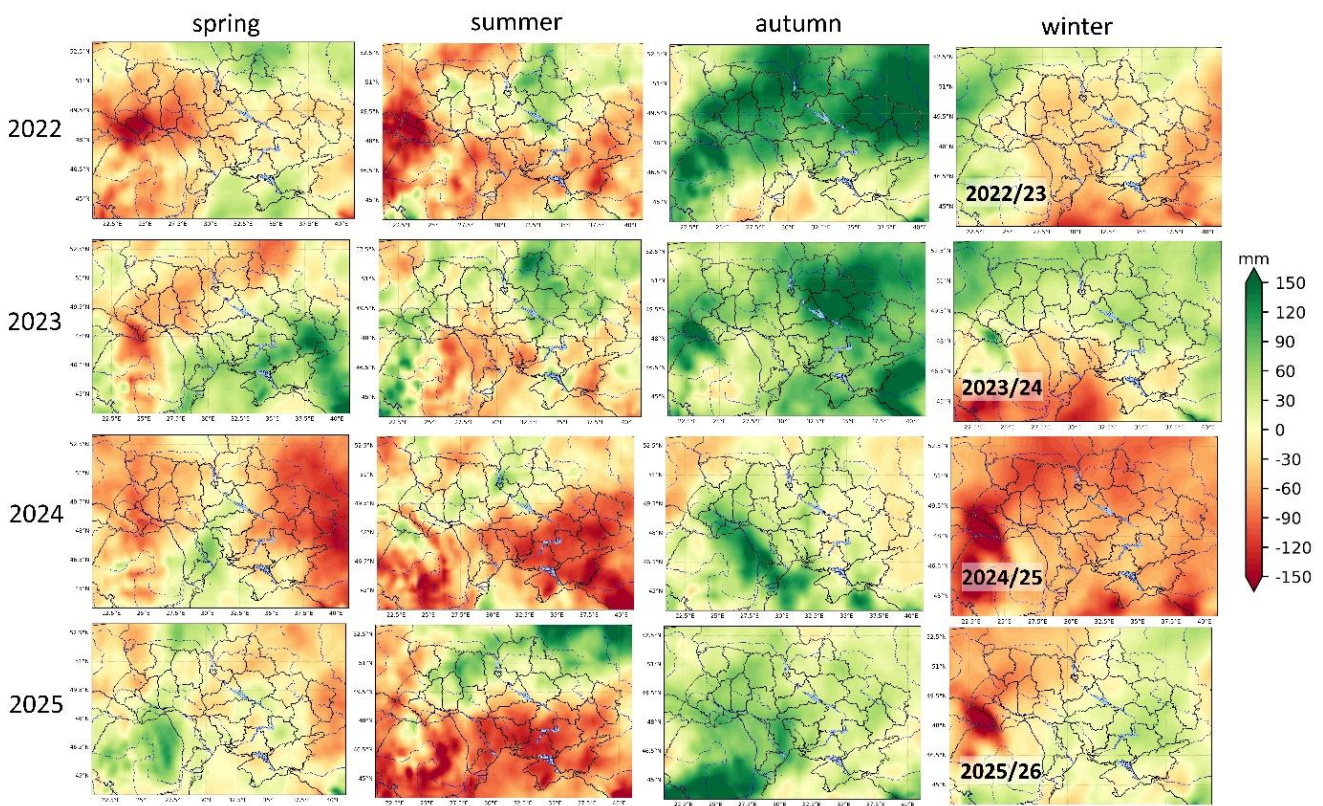


Fig. 2. Changes in the seasonal accumulated precipitation (mm) since the beginning of the full-scale invasion (spring 2022 – winter 2025/2026) compared to the average accumulated precipitation of the corresponding season during the baseline period (2019–2021)

The **boundary layer height**, which indirectly determines the conditions for vertical dispersion of air pollutants and reflects changes in the frequency of atmospheric blocking layer formation, during the period from spring 2022 to winter 2025/26 across Ukraine was generally characterized by higher values in the spring–summer season and lower values in the autumn–winter season compared to the baseline period (2019–2021). [Fig. 3](#) presents the seasonal changes in the mean boundary layer height during the period of the full-scale Russian invasion.

The most significant changes were observed in the summers of 2024 and 2025 in southern Ukraine, where the boundary layer height was 150–300 m higher than in the baseline period. This indicates more favorable dynamical conditions for the dispersion of pollutants from the near-surface layer. Overall, higher boundary layer heights were also observed in summer 2022 in southern Ukraine, as well as in spring 2022, 2023, and 2024.

Less favorable conditions for vertical dispersion of air pollutants were observed in autumn 2022 and 2025, as well as in winter seasons of 2022/23, 2024/25, and 2025/26 in the northern and western regions. During these periods, the boundary layer height was, on average, 50–100 m lower than in the baseline period.

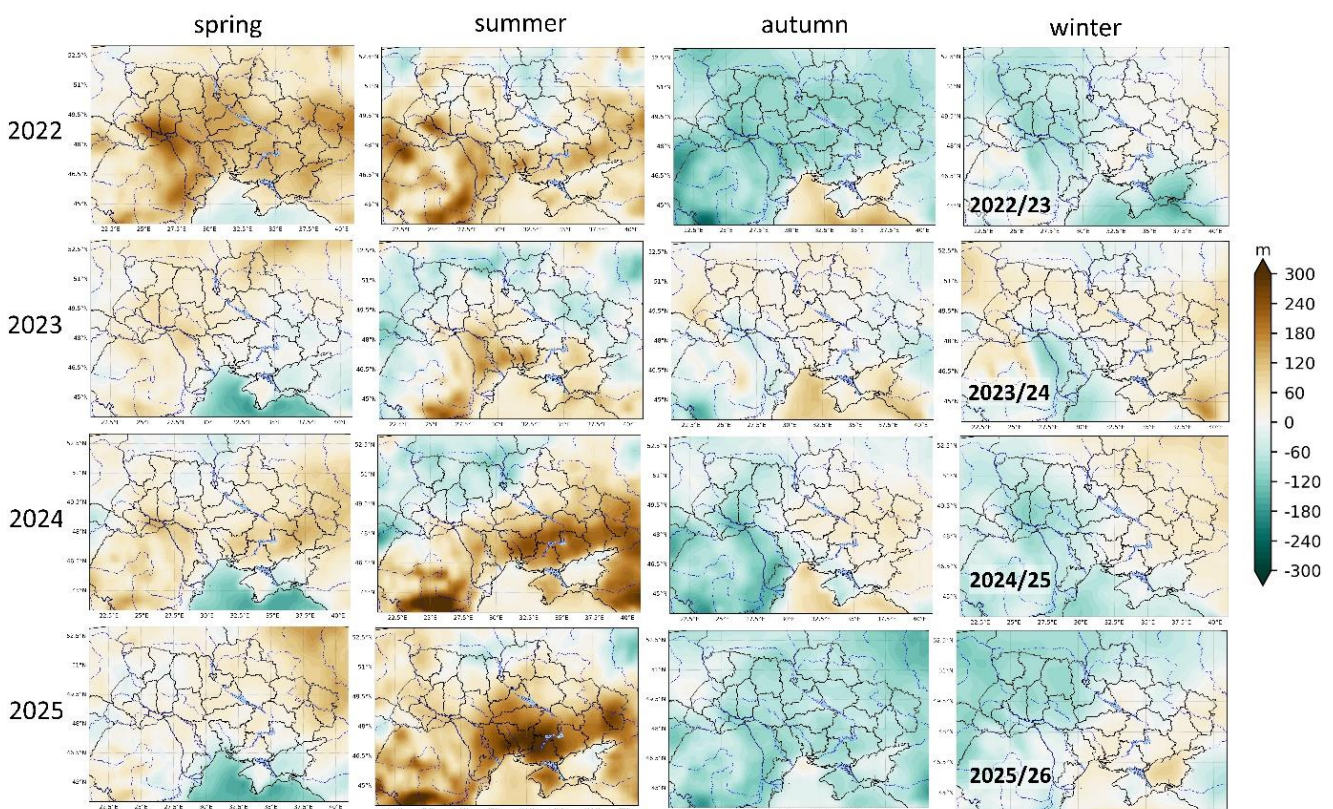


Fig. 3. Changes in the seasonal mean boundary layer height (m) since the beginning of the full-scale invasion (spring 2022 – winter 2025/2026) compared to the mean boundary layer height of the corresponding season during the baseline period (2019–2021)

Near-surface **wind speed** determines the intensity of horizontal dispersion of air pollutants within the near-surface atmospheric layer. During the period from spring 2022 to winter 2025/26 over the territory of Ukraine, an increase in wind speed was predominantly observed in autumn, a decrease in spring, and mixed patterns of change during summer and winter seasons. [Fig. 4](#) presents the seasonal changes in near-surface wind speed during the period of the full-scale Russian invasion.

A decrease in near-surface wind speed creates conditions that favor greater accumulation of air pollutants in the near-surface atmospheric layer. Such conditions were most typical in spring 2023, 2024, and 2025, in winter 2024/25 and 2025/26, and in northern Ukraine during summer 2023 and 2024.

Significant increases in wind speed, associated with more favorable conditions for pollutant dispersion, were observed in autumn 2023 and 2024, in summer 2025, and in winter 2023/24.

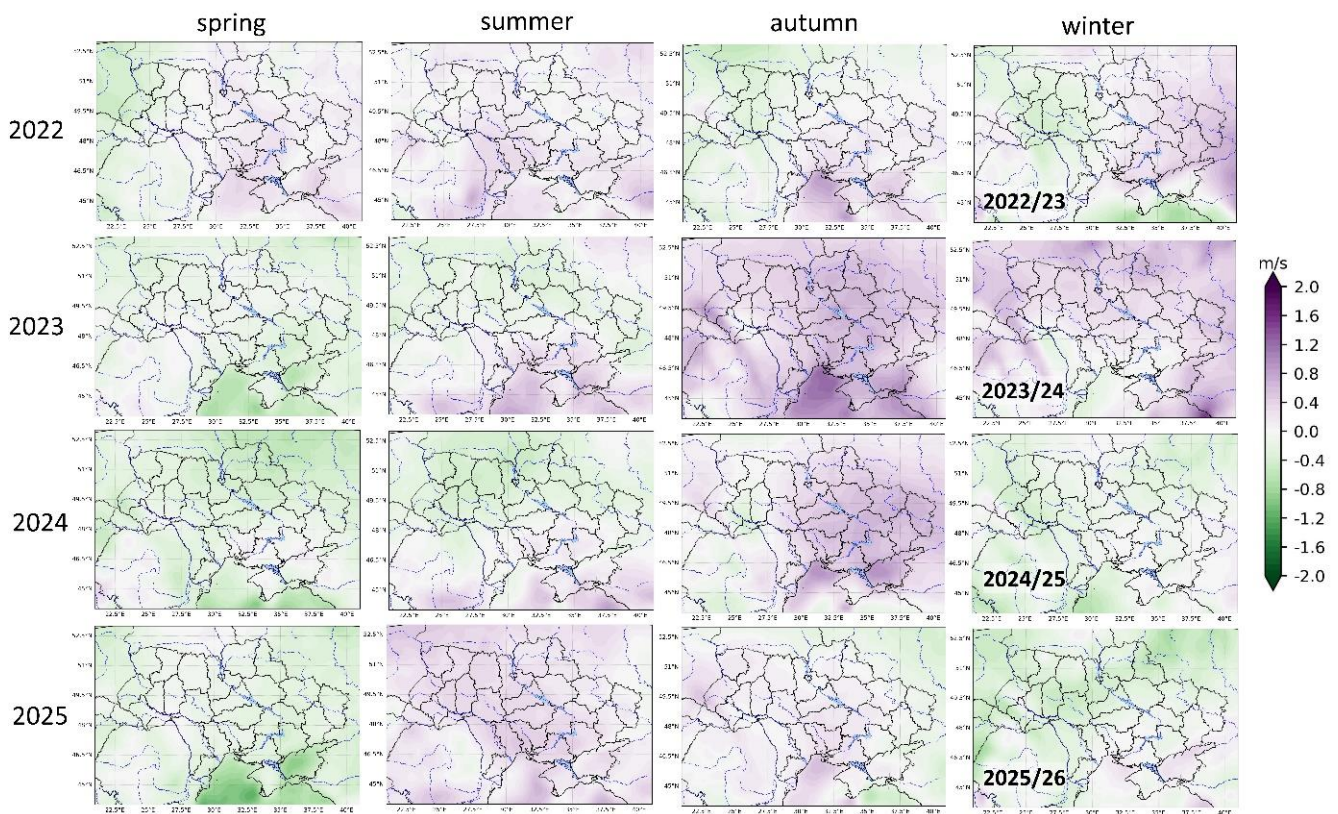


Fig. 4 Changes in the seasonal mean wind speed (m/s) since the beginning of the full-scale invasion (spring 2022 – winter 2025/2026) compared to the mean wind speed of the corresponding season during the baseline period (2019–2021)



# Changes in the distribution of landscape fires

Alongside anthropogenic emissions from industrial facilities and urban transport, landscape fires have always played a significant role in shaping air pollution in Ukraine<sup>7,8,9</sup>. The spatial distribution of landscape fires can be clearly traced using thermal anomaly data from the MODIS (Terra satellite) and VIIRS instruments (Suomi NPP, NOAA-20, NOAA-21), as presented seasonally for the period 2019–2025/26 in [Fig. 5](#).

Before the start of the full-scale Russian invasion, landscape fires exhibited a distinct seasonal pattern<sup>7,8</sup>. In spring, the regular burning of plant remnants in agricultural fields led to the formation of thousands of thermal anomalies, which were clearly detected by satellite observations and covered most of the territory of Ukraine<sup>9</sup>. A similar pattern was observed in autumn, although the number of such fires was lower compared to the spring season. In summer, the distribution of landscape fires across Ukraine was primarily driven by unfavorable meteorological conditions, including high air temperatures and low soil moisture<sup>10</sup>; therefore, most thermal anomalies were observed in the southern and southeastern regions of the country.

With the onset of the full-scale Russian invasion, a redistribution of landscape fires occurred<sup>11,12</sup>. The primary driver became the concentration of fires along the line of active hostilities caused by frequent shelling of military positions. A secondary, but still significant, factor was the reduction in seasonal burning of plant remnants in agricultural fields due to the introduction of stricter enforcement during wartime<sup>13</sup>.

Immediately after the beginning of hostilities and active combat operations, the spatial pattern of thermal anomalies began to clearly delineate the front line. In particular, in spring 2022, the highest occurrence of landscape fires was observed in eastern Ukraine and in the Kyiv region. In summer 2022, landscape fires were distributed along the front line extending from the southern part of Kherson region to the northern part of Kharkiv region. The period from autumn 2022 to spring 2023 was the last interval during which the number of thermal anomalies during the warm season along the front line remained relatively low. Starting from summer 2023, landscape fires along the front line have consistently formed pronounced hotspots and have become a major source of biomass burning emissions.

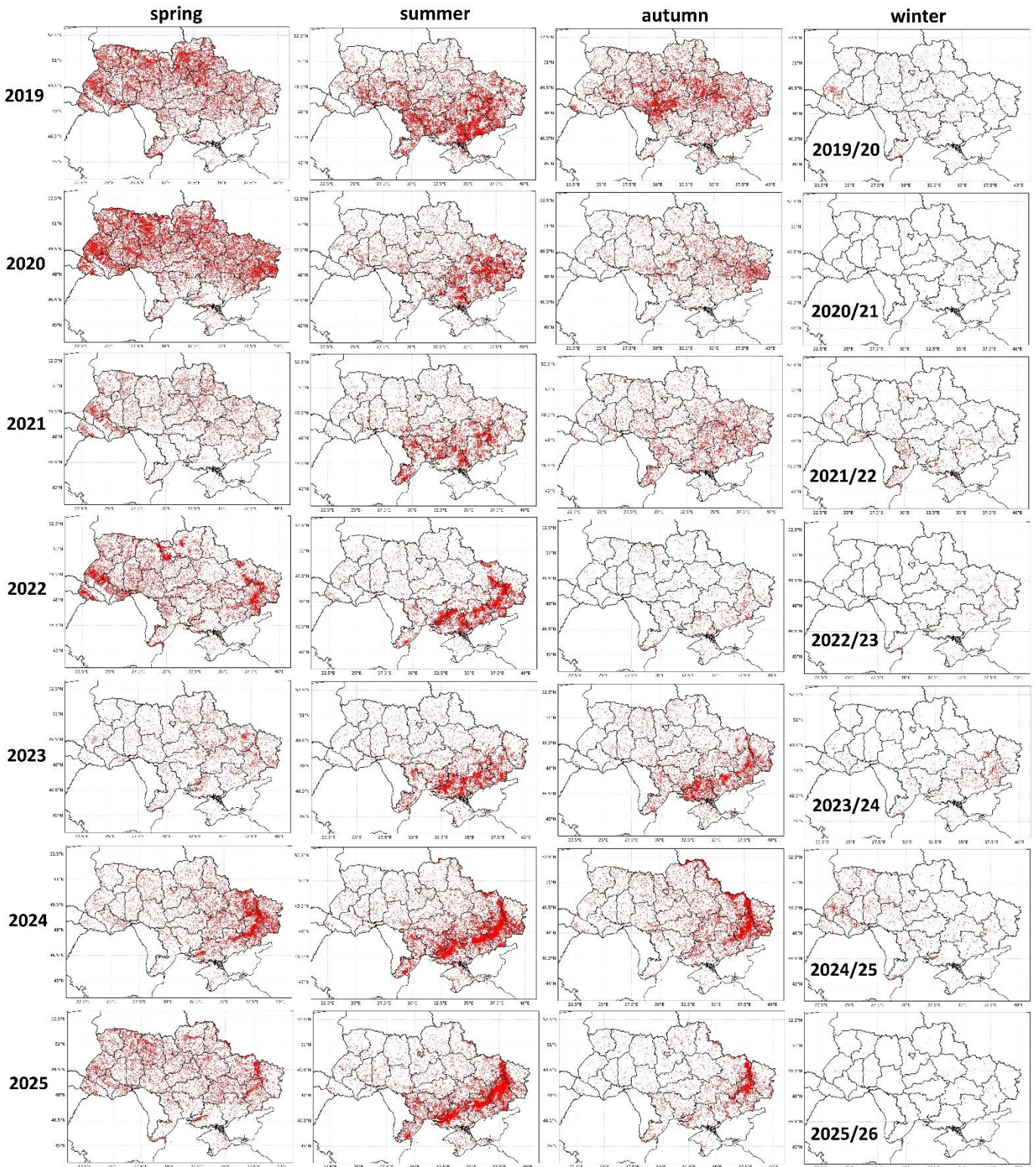


Fig. 5. Spatial distribution of heat anomalies detected by the MODIS and VIIRS satellite sensors from spring 2019 to winter 2025/2026.

A large, billowing mushroom cloud from a nuclear explosion dominates the sky. The top of the cloud is bright orange and yellow, while the lower part is dark and smoky. A thick column of dark smoke and debris rises from the ground, supporting the cloud. The background shows a clear blue sky with some light clouds and a distant horizon with hills and fields.

**Changes in air  
quality.**

**Short-term impacts**

The primary consequence of military activity for air quality is a sharp, relatively short-term increase in pollutant concentrations in the atmosphere due to emissions following missile and drone strikes (or other war-related emergency events). Before the war, such emissions were extremely rare and typically associated with industrial accidents; however, during the war, these events have become a regular occurrence. Due to the ability of the atmosphere to rapidly remove most pollutants, the duration of elevated pollution levels does not exceed several hours after the cessation of the emission source activity (e.g., after an explosion or complete extinguishing of a fire). At the same time, despite their short duration, the magnitude of these emissions is such that pollutant concentrations may pose an immediate risk to human health if populations are located within the plume dispersion area.

During the period of the full-scale invasion, thousands of missile and drone strikes have been recorded, leading to the formation of strong emissions of hazardous substances. However, the detection of such events by any ground-based monitoring system is largely incidental, as it requires both temporal (measurements taken during or shortly after the emission event) and spatial (measurements aligned with the transport of the emission plume by wind) coincidence between the emission source and the monitoring station location. As a result, given the point-based nature of ground observations, air pollution associated with most missile and drone strikes remains undetected.

For the period from 2022 to 2025, a total of 443 cases were identified in which elevated concentrations measured at stationary monitoring stations of hydrometeorological organizations coincided with the impacts of missile and drone strikes on Ukrainian cities ([Fig. 6](#)). Considering the total number of attacks, the detection rate of direct concentration increases associated with strikes is less than 1%. In the first two years of the full-scale invasion, only 60 cases (2022) and 42 cases (2023) were identified. The increase in the number of missiles and drones launched against Ukraine in 2024 and 2025 led to a rise in the number of short-term episodes of strong pollutant emissions. In 2024, 153 such cases were identified, and in 2025, 188 cases of increased pollutant concentrations were detected that can be directly attributed to military activity rather than other factors such as routine urban emissions, landscape fires, or unfavorable meteorological conditions for atmospheric self-cleaning.

[Fig. 6](#) shows the annual distribution of confirmed air pollution episodes based on monitoring station data, as well as the average exceedances of pollutant concentrations following missile and drone strikes relative to pre-event levels. These estimates are based on TSP, CO, SO<sub>2</sub>, and NO<sub>2</sub> – the pollutants with the highest observational coverage in Ukraine.

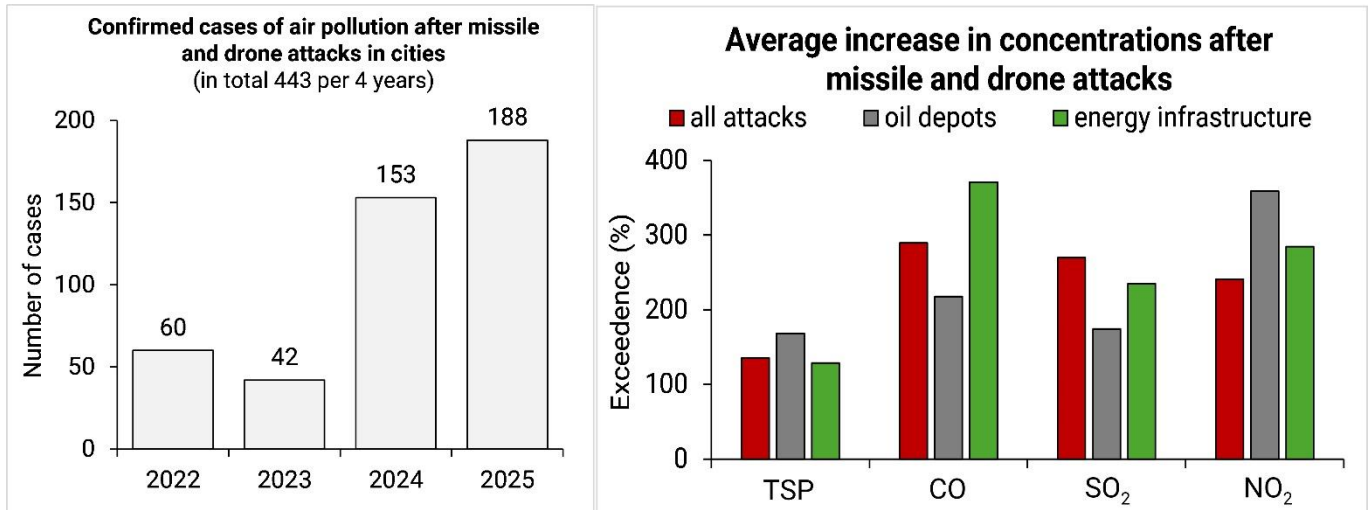


Fig. 6. Annual distribution of confirmed air pollution events based on monitoring station data, and average exceedances of pollutant concentrations in the immediate period following missile or drone strikes relative to pre-strike levels for TSP, carbon monoxide (CO), sulfur dioxide (SO<sub>2</sub>), and nitrogen dioxide (NO<sub>2</sub>).

Following missile and drone strikes on cities, average concentrations of air pollutants increased by 135% for TSP, 240% for NO<sub>2</sub>, 270% for SO<sub>2</sub>, and 290% for CO (fig. 6). For all considered pollutants, extreme cases of severe air pollution led to concentration increases of more than 1000% relative to pre-attack levels. The analysis and interpretation of these results require consideration of the fact that the conditions under which exceedances are identified are not homogeneous and, in general, cannot be compared using standard statistical approaches. First, the monitoring station recording increased concentrations may in some cases be located close to the impact site, while in others it may be several kilometres away. Second, measurements may be taken immediately after the strike in some cases, and several hours later in others. Therefore, all reported relative changes in pollution represent only aggregated effects intended to illustrate the general magnitude of concentration increases following missile and drone attacks, and do not provide precise estimates of exceedances under specific conditions.

When considering differences in impacts between strikes on energy infrastructure and those on oil storage facilities and refineries, CO and SO<sub>2</sub> concentrations were, on average, higher following strikes on energy facilities, whereas TSP and NO<sub>2</sub> showed greater increases associated with fires at oil depots and refineries. As with the overall assessment of all cases, this pattern reflects aggregated observational outcomes and does not demonstrate a strictly causal relationship indicating more intense increases of specific pollutants under one type of strike compared to another.

Despite all advantages of satellite remote sensing related to the coverage of areas without ground-based observations and regions of active hostilities, the analysis of four years of the full-scale Russian invasion has demonstrated the limited capability for quantitative assessment of air pollutant content during short-term air quality deterioration events, particularly following missile and drone strikes. While satellite remote sensing of thermal anomalies and the Earth's surface allows more frequent and reliable detection of the impacts of missile strikes and landscape fires, the estimation of pollutant concentrations is constrained by the relatively low accuracy of atmospheric retrievals and the insufficient number of available satellites for this purpose.

Polar-orbiting satellites, which provide only one observation per day during daytime hours, most often failed to capture the majority of war-related emission sources, particularly those occurring during night-time and early morning missile and drone strikes. While landscape fires near the front line are more frequently detected, the impacts of missile and drone strikes on urban air pollutant concentrations are often indistinguishable from background anthropogenic emissions unrelated to military activity (transport and industry). When combined with frequent cloud cover that hinders satellite observations, the number of cases in which quantitative changes in pollution can be reliably assessed becomes critically small.

The launch of the geostationary Sentinel-4 satellite may significantly improve detection capabilities starting from 2026; however, satellite air quality monitoring during the first four years of the war will remain fundamentally limited in terms of capturing the impacts of missile and drone strikes.

Previous scientific studies<sup>14</sup> have presented examples of short-term deterioration in air quality associated with industrial facilities. Since a significant number of missile and drone strikes are directed at urban infrastructure, their impacts are only rarely distinguishable against the background of urban pollution, especially considering the substantial time lag between the strike and satellite overpass. This time lag is often longer than the atmospheric lifetime of  $\text{NO}_2$ , which is the most suitable pollutant for quantitatively assessing the impacts of such events.

[Fig. 7](#) presents an example of a large-scale missile strike on Kyiv that occurred on 8 July 2024 between approximately 10:00 and 13:00 local time. Because the strike occurred shortly before the Sentinel-5P satellite overpass, its impacts on atmospheric pollution can be quantitatively assessed. During this missile attack, a strike hit the "Okhmatdyt" children's hospital, destroyed an entrance of a five-story residential building, and impacted multiple sites across seven districts of Kyiv.

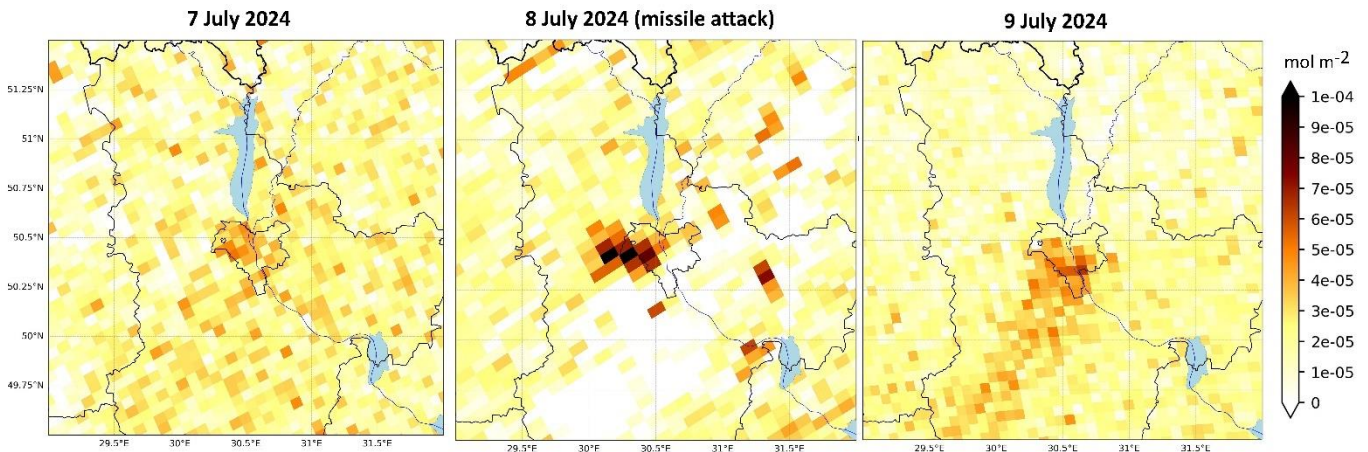


Fig. 7. Spatial distribution of nitrogen dioxide ( $\text{NO}_2$ ) over Kyiv on 7, 8, and 9 July 2024 (8 July – day of the missile strike) based on TROPOMI satellite instrument data

According to satellite data, the impacts of missile and drone strikes are most often observed as short-term and abrupt exceedances of air pollutant concentrations. During these events, the increase in the VCD of the analyzed pollutant averages between 100% and 200% compared to mean background levels (or air conditions of the preceding days). The vast majority of such effects are detected for  $\text{NO}_2$ , while a smaller number of cases associated with active combustion allow for the detection of increases in CO and particulate matter. In satellite remote sensing, particulate matter cannot be directly quantified and is instead indirectly assessed using aerosol optical depth and the absorbing aerosol index. Over the four years of the full-scale invasion, satellite observations did not allow for the identification of any cases of increased  $\text{SO}_2$  and  $\text{CH}_2\text{O}$  that could be reliably attributed to missile or drone strikes. This is primarily due to the previously mentioned limitations related to retrieval accuracy for these chemical species, frequent cloud cover, and the significant time lag between most strikes and polar-orbiting satellite overpasses. For  $\text{SO}_2$  and  $\text{CH}_2\text{O}$ , ground-based monitoring provides substantially more reliable and informative evidence of short-term concentration increases.

In general, the assessment of air pollution impacts (when detected by satellites) following Russian attacks on Ukrainian cities and industrial facilities appears as anomalously high concentrations of pollutants. As illustrated in [Fig. 7](#),  $\text{NO}_2$  VCD in the polluted urban air plume over Kyiv were 2–2.5 times higher after the missile strikes on 8 July 2024 compared to typical city conditions on 7 and 9 July 2024.

During landscape fires, satellite monitoring is capable of detecting short-term increases in CO and tracking polluted air plumes originating from fire locations. [Fig. 8](#) shows an example of CO transport associated with landscape fires on 30 July 2025, caused by shelling along the front line.

It is evident that the sensitivity of detecting enhancements in CO VCD over a relatively homogeneous spatial background depends on the intensity and magnitude of biomass burning. Therefore, most observed landscape fire events do not produce

detectable changes in the total atmospheric column. Under conditions where background CO values range from 0.023 to 0.035 mol/m<sup>2</sup>, clear fire-related enhancements can be identified when total CO exceeds 0.040–0.045 mol/m<sup>2</sup> (depending on the season). Short-term CO enhancements along the front line during landscape fires are approximately 30–70% relative to background values in unaffected areas. During particularly intense fires, CO may exceed 0.065 mol/m<sup>2</sup>, corresponding to increases of 100–150% above background levels.

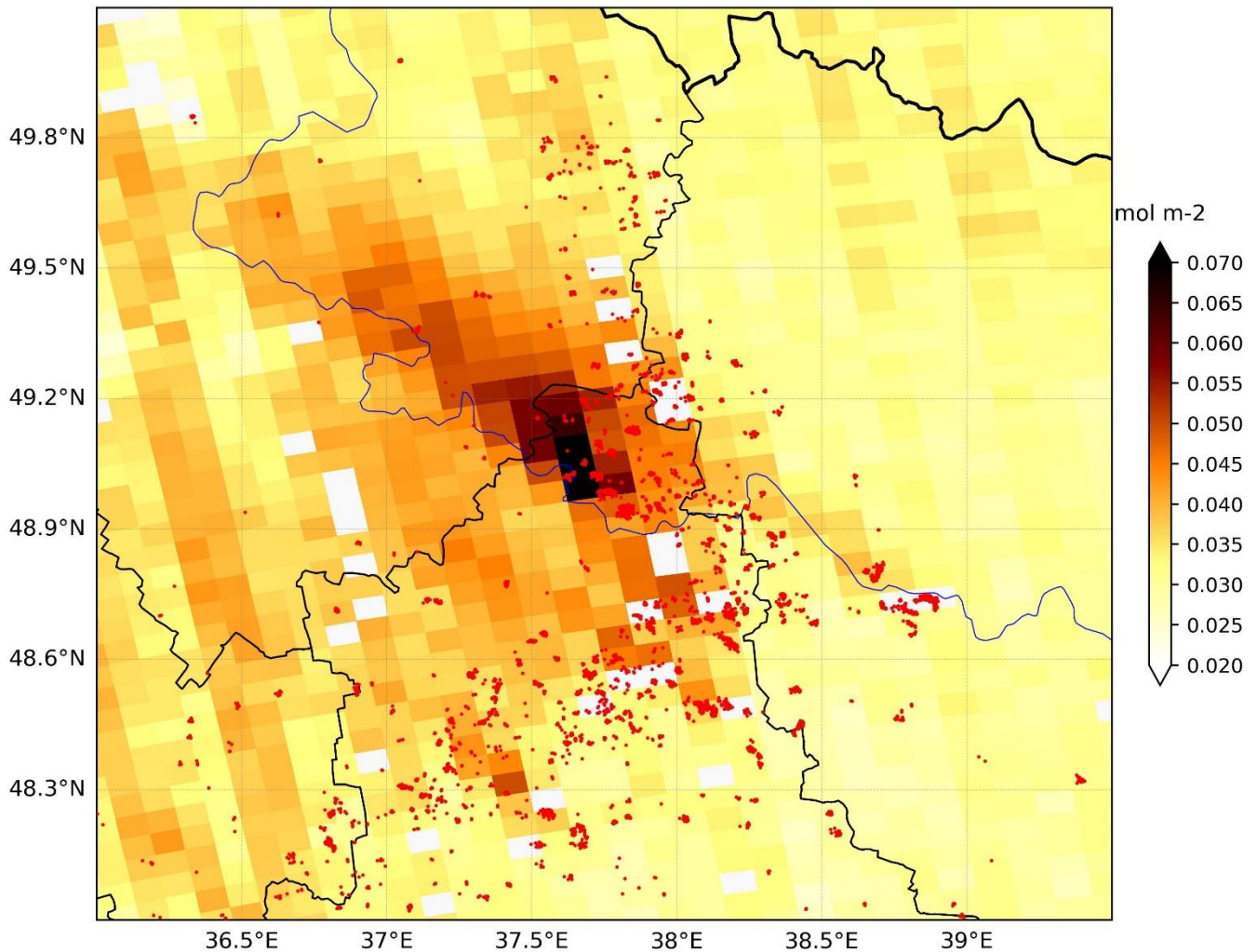


Fig. 8. Spatial distribution of carbon monoxide (CO) based on TROPOMI satellite instrument data and thermal anomalies from MODIS and VIIRS satellite instruments along the front line in Kharkiv, Luhansk, and Donetsk regions on 30 July 2025.

A photograph of a sunset over a river. The sky is filled with orange and yellow clouds, and the sun is low on the horizon. A tall, dark chimney is visible in the background, and its reflection is seen in the water. The river is calm, and the surrounding trees are silhouetted against the sky.

**Changes in air  
quality.**

**Long-term effects**

The previously considered short-term effects of military activities on air quality are unidirectional and reflect an immediate deterioration of atmospheric conditions following missile and drone strikes. However, on a multi-year scale, changes in air quality reflecting the long-term effects of war are far more complex and include the combined influence of a large number of processes that often have opposing impacts on pollution levels. In addition to the high frequency of short-term episodes of severe pollution caused by missile strikes and ecosystem fires along the front line, socio-economic consequences also begin to play an increasingly important role. The main war-related drivers contributing to increased concentrations of air pollutants include:

- missile and drone strikes, and explosions resulting from sabotage activities;
- landscape fires following shelling;
- damage to military equipment and other infrastructure in active combat zones;
- changes in fuel types and fuel usage;
- increased vehicle emissions in areas receiving internally displaced populations;
- operation of generators during power outages;
- increased emissions from military vehicles near the front line; among others.

At the same time, several processes contribute to reductions in pollutant emissions, including:

- shutdown and destruction of industrial facilities;
- reduced vehicle emissions due to population displacement;
- reduced seasonal agricultural open burning due to stricter enforcement;
- temporary suspension of industrial activity during blackouts.

Most of these processes occur simultaneously, against the background of changing prevailing meteorological conditions that determine the atmospheric capacity for pollutant removal. This makes the long-term effects of military activity on air quality highly complex and heterogeneous in their impacts.

Analysis of pollutant concentrations based on ground-based monitoring data from hydrometeorological organizations has revealed the spatially localized nature of air pollution changes during the full-scale Russian invasion, their dependence on the economic role of cities and existing industrial activity, proximity to the front line, as well as differing trends among various chemical species.

Based on the analyzed trends in ground-level air pollution, three main long-term effects of military actions can be identified:

- 1) an increase in air pollution in frontline cities, directly associated with active military operations;

- 2) a decrease in average pollution levels in large industrial cities, primarily due to the destruction of industrial facilities;
- 3) a redistribution of pollutant concentrations in rear-area cities.

Air pollution in most major Ukrainian cities was primarily formed by key pollutants—CO, NO<sub>2</sub>, and particulate matter (in form of TSP)<sup>15</sup>. Four years of Russia's full-scale invasion (2022–2026), accompanied by regular missile strikes on industrial facilities, resulted in a predominant decrease (with some exceptions) in the concentrations of these pollutants in cities such as Dnipro, Horishni Plavni, Kharkiv, Kremenchuk, Kryvyi Rih, Kyiv, Odesa, Zaporizhzhia, and others (see [Figs. 9, 11, 13](#)). In contrast, in Kramatorsk and Sloviansk, located close to active combat zones, concentrations of CO, NO<sub>2</sub>, and TSP increased on average by 12–40%, depending on the city and pollutant. Increases in NO<sub>2</sub> and TSP within a wide range of 15% to 87% were also recorded in cities near the front line and border areas, including Kherson, Sumy, and Chernihiv. Being closely related in emission sources, soot ([Fig. 14](#)) and NO ([Fig. 12](#)) largely followed trends similar to TSP and NO<sub>2</sub>, respectively, varying within a range of -25% to 35%.

In more distant rear-area cities, changes in CO, NO<sub>2</sub>, and TSP concentrations were heterogeneous. An increase in CO was recorded in Ivano-Frankivsk, Kropyvnytskyi, Ternopil and Zhytomyr ; an increase in NO<sub>2</sub> in Bila Tserkva and Poltava; and an increase in TSP in Obukhiv, Uzhhorod, Zhytomyr, and others. A decreasing trend in CO concentrations was observed in Bila Tserkva, Brovary, Khmelnytskyi, Obukhiv and Uzhhorod; a decrease in NO<sub>2</sub> in Cherkasy, Chernivtsi, Khmelnytskyi, Obukhiv, Vinnytsia; and a decrease in TSP in Bila Tserkva, Chernivtsi, Ternopil, and several other cities.

In Ukraine, the formation of SO<sub>2</sub> concentrations was associated with the operation of TPPs/CHPs as well as metallurgical, coke-chemical, and chemical industries. During the period of Russia's full-scale invasion, three main patterns of SO<sub>2</sub> concentration changes were identified ([Fig. 10](#)). The first pattern is a decrease in SO<sub>2</sub> by 11–16% in several industrial cities where levels were historically high, including Dnipro, Kamianske, Odesa, and Sloviansk. The second pattern is an increase of 29–63% in other industrial cities, such as Kryvyi Rih and Svitlovodsk, including those located closer to the border or front line (Kharkiv, Kherson, Sumy). The third pattern is a substantial decrease in SO<sub>2</sub> — on average by 30–60% in cities in Western Ukraine, including Chernivtsi, Ivano-Frankivsk, Khmelnytskyi, and Lviv. Exceptions include Lutsk and Uzhhorod, where SO<sub>2</sub> increased relative to the baseline period of 2019–2021. Thus, there is an overlap of opposing effects associated with the destruction of TPPs/CHPs and industrial facilities (leading to a decrease in SO<sub>2</sub>), and the increased use of generators and fuel types with higher pollutant content (leading to an increase in SO<sub>2</sub>).

Concentrations of C<sub>6</sub>H<sub>5</sub>OH increased on average by 10–15% during the full-scale invasion in cities experiencing regular shelling or located near active combat zones,

including Kharkiv, Kherson, Kramatorsk and Sloviansk (with Lutsk as an exception, where changes in  $C_6H_5OH$  trends are likely unrelated to military activity) (see [Fig. 15](#)). In large industrial cities,  $C_6H_5OH$  decreased on average by 20–40%.

In comparison to  $C_6H_5OH$ , the trends in  $CH_2O$  during the full-scale Russian invasion are significantly more heterogeneous and more difficult to attribute to specific driving factors ([Fig. 16](#)). In cities close to the front line or border areas (Izmail, Kherson, Kramatorsk, Sloviansk, Sumy, Zaporizhzhia), an increase in  $CH_2O$  of 12–35% was observed. In industrial cities located farther from active combat zones, a general decrease in  $CH_2O$  concentrations was recorded (Dnipro, Kremenchuk, Kryvyi Rih, Mykolaiv, Odesa, etc.), although opposite trends were observed in some cases (e.g., Svitlovodsk). In rear-area cities, the patterns are highly heterogeneous.

In industrial cities with previously higher  $NH_3$  concentrations, a decrease of 10–25% was observed during the full-scale invasion, particularly in Cherkasy, Kamianske, Kremenchuk, Kryvyi Rih and Kyiv ([Fig. 17](#)), indicating a decline in industrial production. A slight increase in  $NH_3$  was observed in Kharkiv, Poltava and Rivne, and a more pronounced increase in Vinnytsia; however, these changes could not be unambiguously linked to the consequences of the war.

Among other specific pollutants, a decrease in  $H_2S$  concentrations of 16–42% was also recorded in industrial cities located away from the front line, particularly in Kamianske, Kryvyi Rih, Kyiv and Odesa ([Fig. 18](#)). In contrast, increases in  $H_2S$  were observed in Cherkasy and Zaporizhzhia. For  $HCl$  concentrations, data from six cities show that a decrease was observed only in Chernivtsi ([Fig. 19](#)), while increases of 8–32% were recorded in Khmelnytskyi, Kyiv, Poltava, Rivne and Zaporizhzhia. For  $HF$  concentrations, one of the most notable trends is a 117% increase in Sloviansk ([Fig. 20](#)), which may be exclusively attributable to the impact of military activity. A decrease of more than 50% in  $HF$  was recorded in Chernivtsi and Kyiv.

## CO

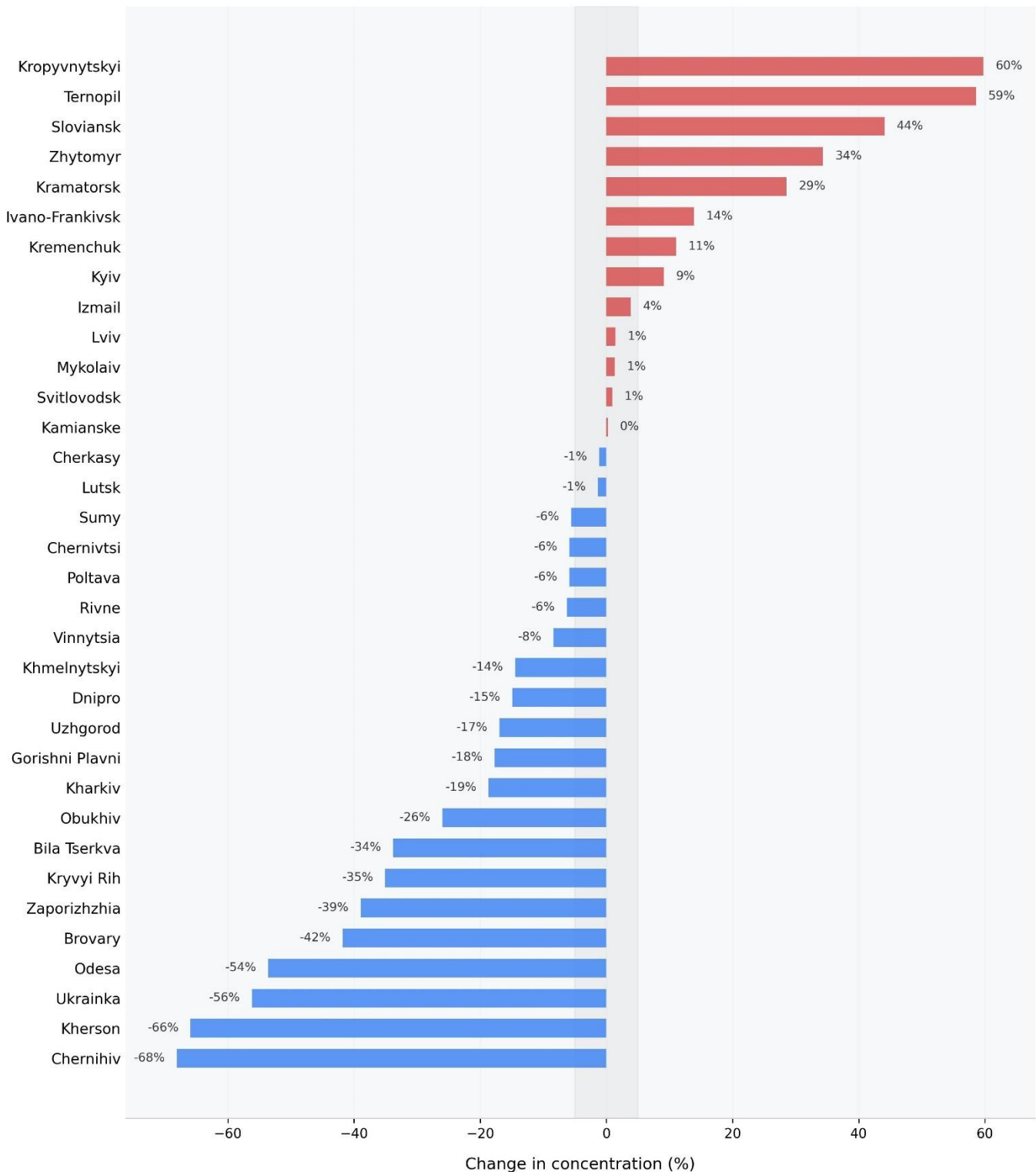


Fig. 9. Percentage change in average concentrations of carbon monoxide (CO) in atmospheric air based on ground-based monitoring data during the period of the full-scale invasion (March 2022 – December 2025), compared with average concentrations for the baseline period (2019–2021) \*

\* Note on result interpretation: the values shown in the plot represent aggregated changes in local pollution within the locations of monitoring stations, which may not correspond to overall patterns for the entire city or its individual districts.

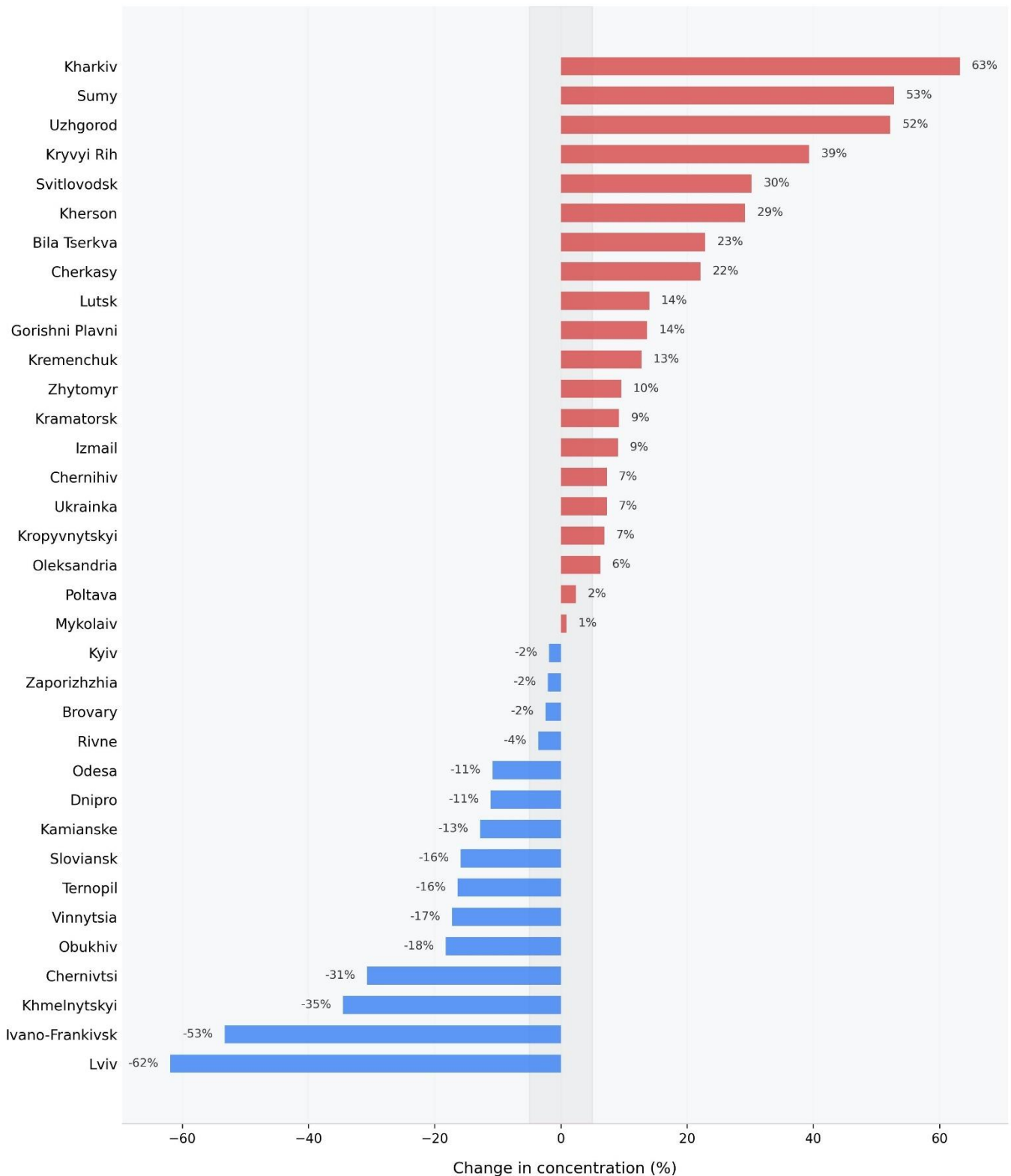
SO<sub>2</sub>

Fig. 10. Percentage change in average concentrations of sulfur dioxide (SO<sub>2</sub>) in atmospheric air based on ground-based monitoring data during the period of the full-scale invasion (March 2022 – December 2025), compared with average concentrations for the baseline period (2019–2021) \*

\* Note on result interpretation: the values shown in the plot represent aggregated changes in local pollution within the locations of monitoring stations, which may not correspond to overall patterns for the entire city or its individual districts.

## NO<sub>2</sub>

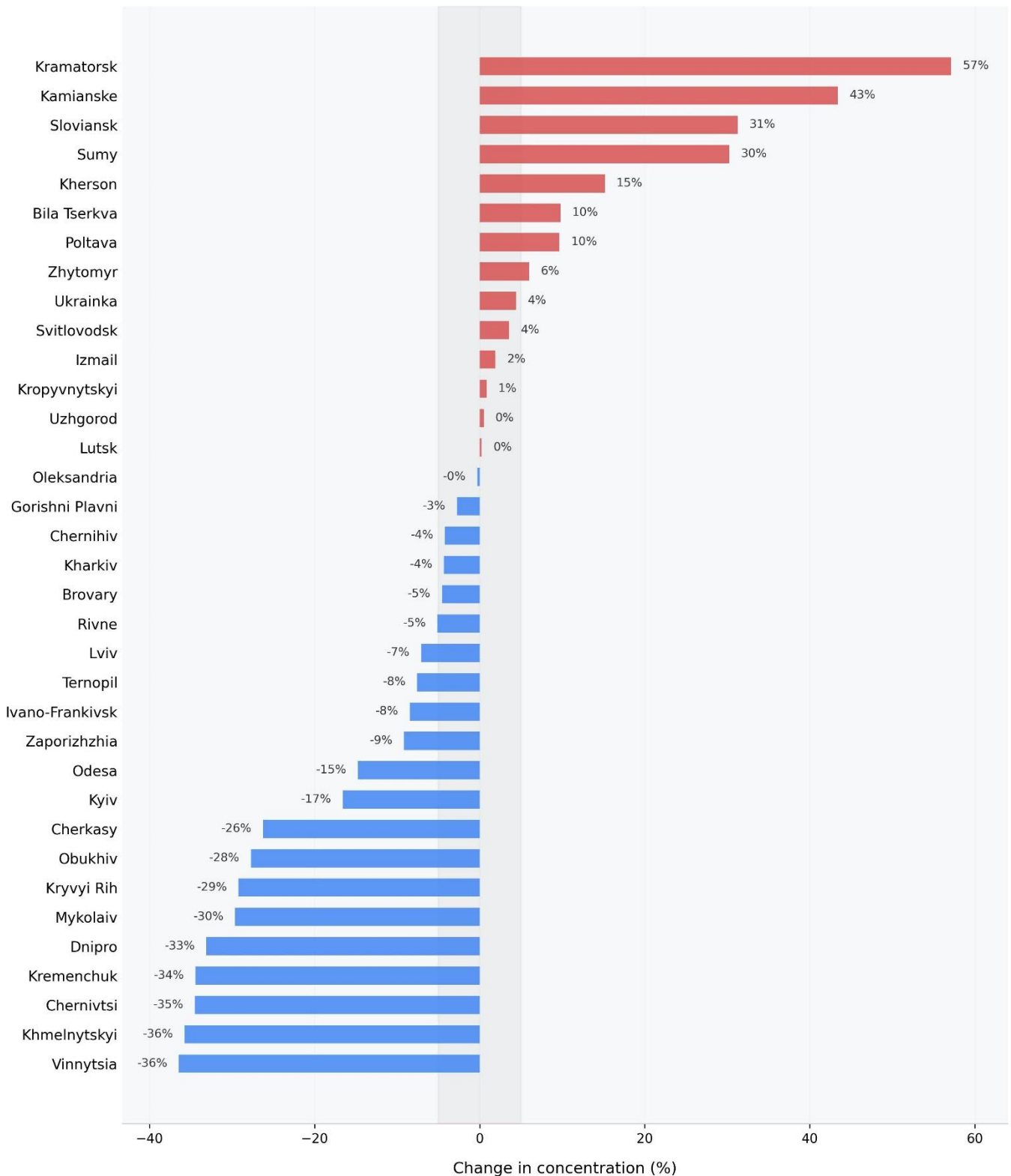


Fig. 11. Percentage change in average concentrations of nitrogen dioxide (NO<sub>2</sub>) in atmospheric air based on ground-based monitoring data during the period of the full-scale invasion (March 2022 – December 2025), compared with average concentrations for the baseline period (2019–2021) \*

\* Note on result interpretation: the values shown in the plot represent aggregated changes in local pollution within the locations of monitoring stations, which may not correspond to overall patterns for the entire city or its individual districts.

## NO

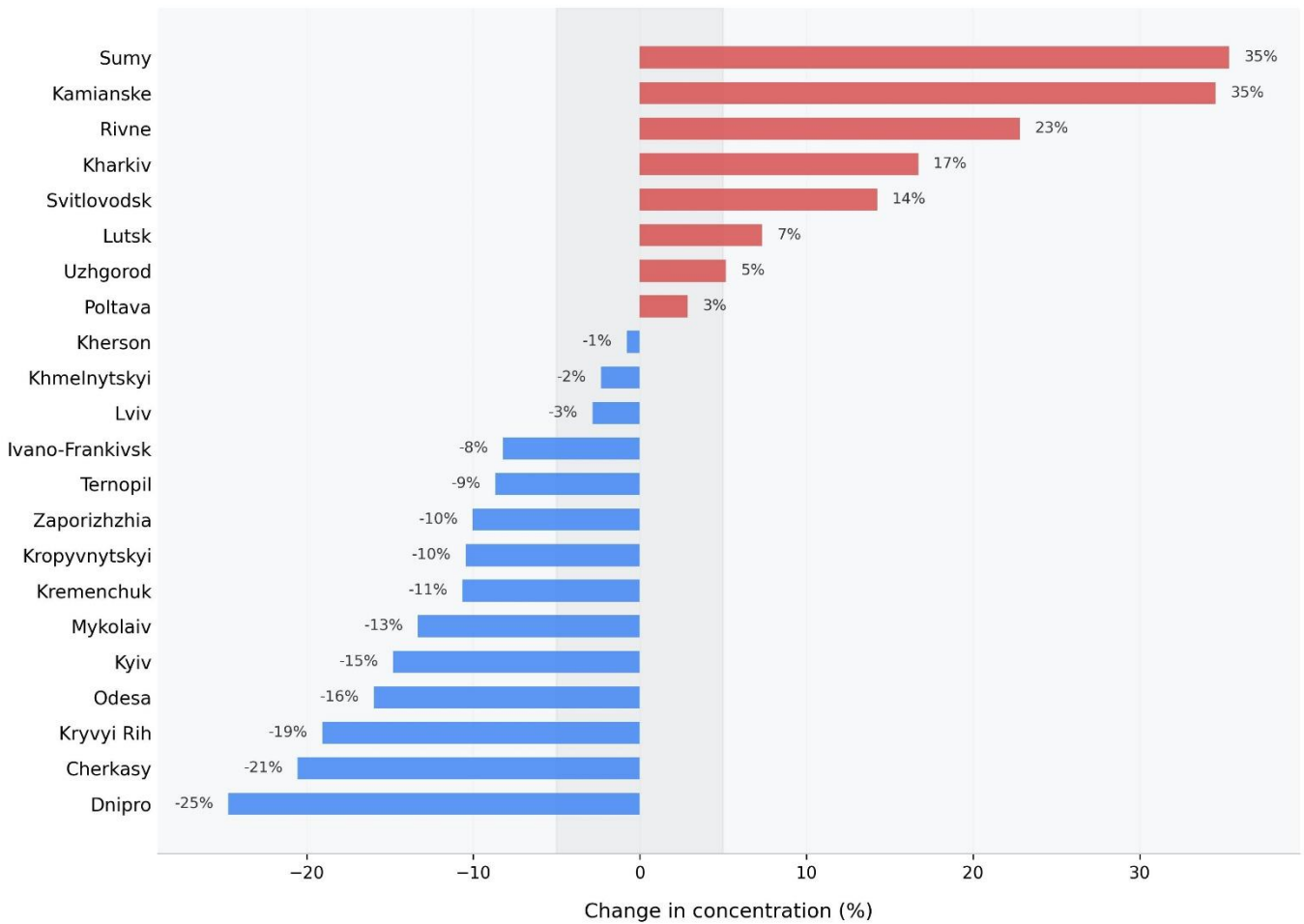


Fig. 12. Percentage change in average concentrations of nitrogen oxide (NO) in atmospheric air based on ground-based monitoring data during the period of the full-scale invasion (March 2022 – December 2025), compared with average concentrations for the baseline period (2019–2021) \*

\* Note on result interpretation: the values shown in the plot represent aggregated changes in local pollution within the locations of monitoring stations, which may not correspond to overall patterns for the entire city or its individual districts.

## TSP

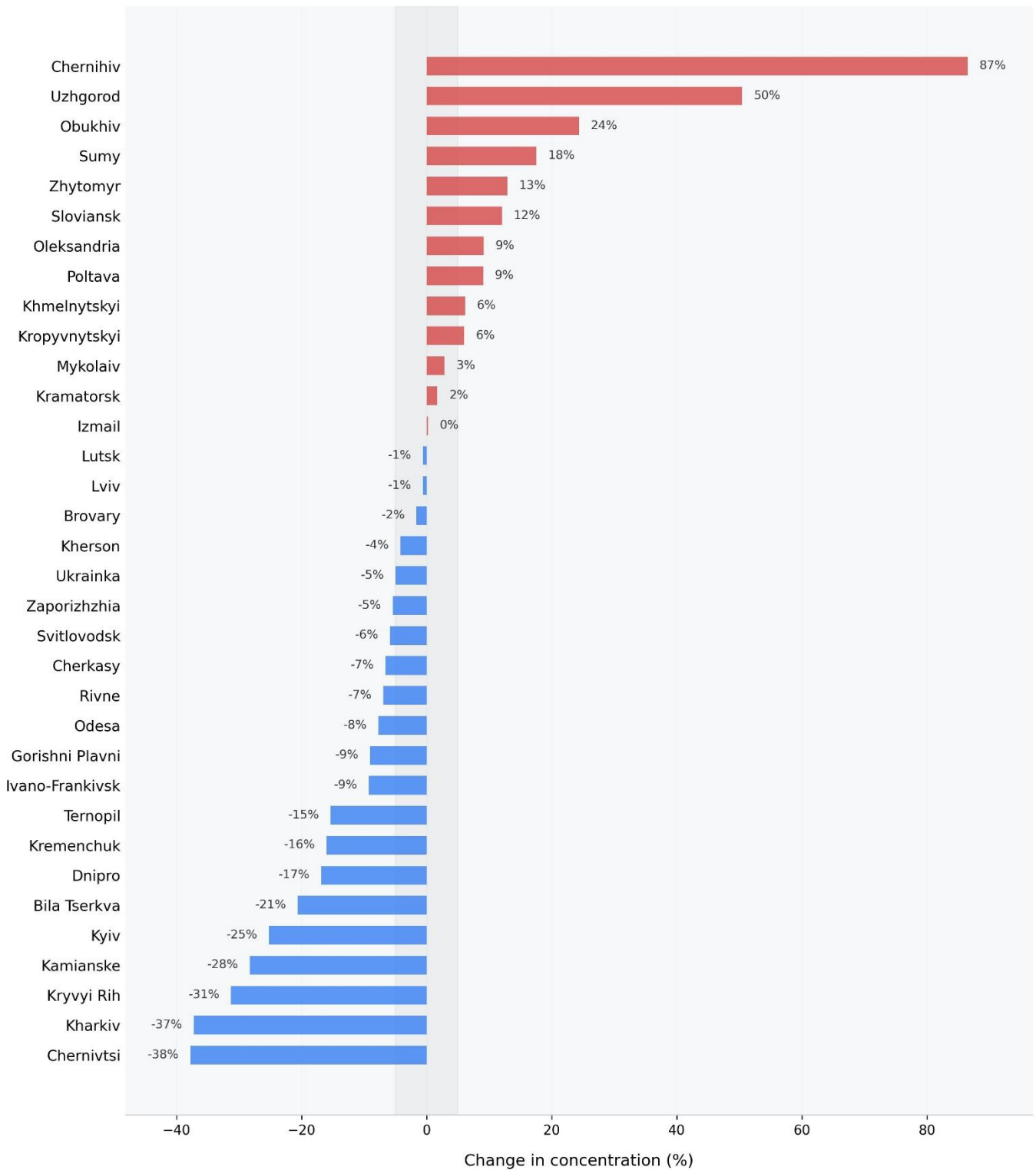


Fig. 13. Percentage change in average concentrations of total suspended particles (TSP) in atmospheric air based on ground-based monitoring data during the period of the full-scale invasion (March 2022 – December 2025), compared with average concentrations for the baseline period (2019–2021) \*

\* Note on result interpretation: the values shown in the plot represent aggregated changes in local pollution within the locations of monitoring stations, which may not correspond to overall patterns for the entire city or its individual districts.

## Soot

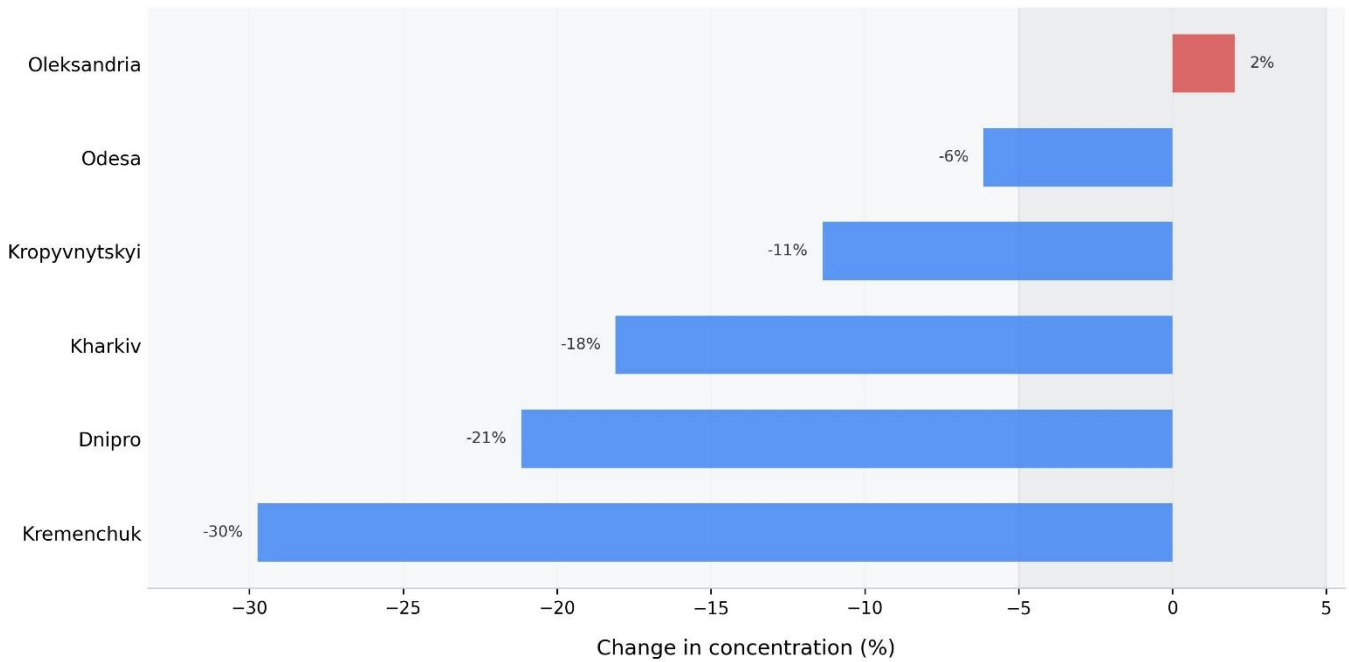


Fig. 14. Percentage change in average concentrations of soot in atmospheric air based on ground-based monitoring data during the period of the full-scale invasion (March 2022 – December 2025), compared with average concentrations for the baseline period (2019–2021) \*

## C<sub>6</sub>H<sub>5</sub>OH

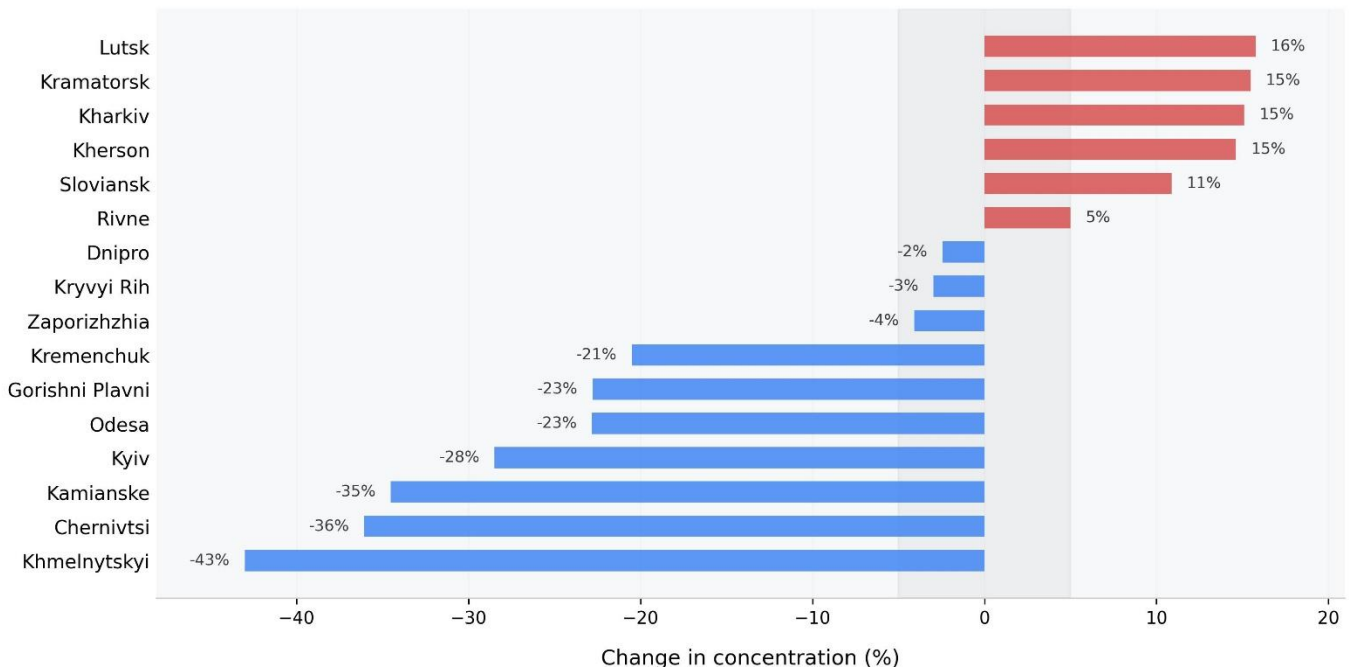


Fig. 15. Percentage change in average concentrations of phenol (C<sub>6</sub>H<sub>5</sub>OH) in atmospheric air based on ground-based monitoring data during the period of the full-scale invasion (March 2022 – December 2025), compared with average concentrations for the baseline period (2019–2021) \*

\* Note on result interpretation: the values shown in the plot represent aggregated changes in local pollution within the locations of monitoring stations, which may not correspond to overall patterns for the entire city or its individual districts.

## CH<sub>2</sub>O

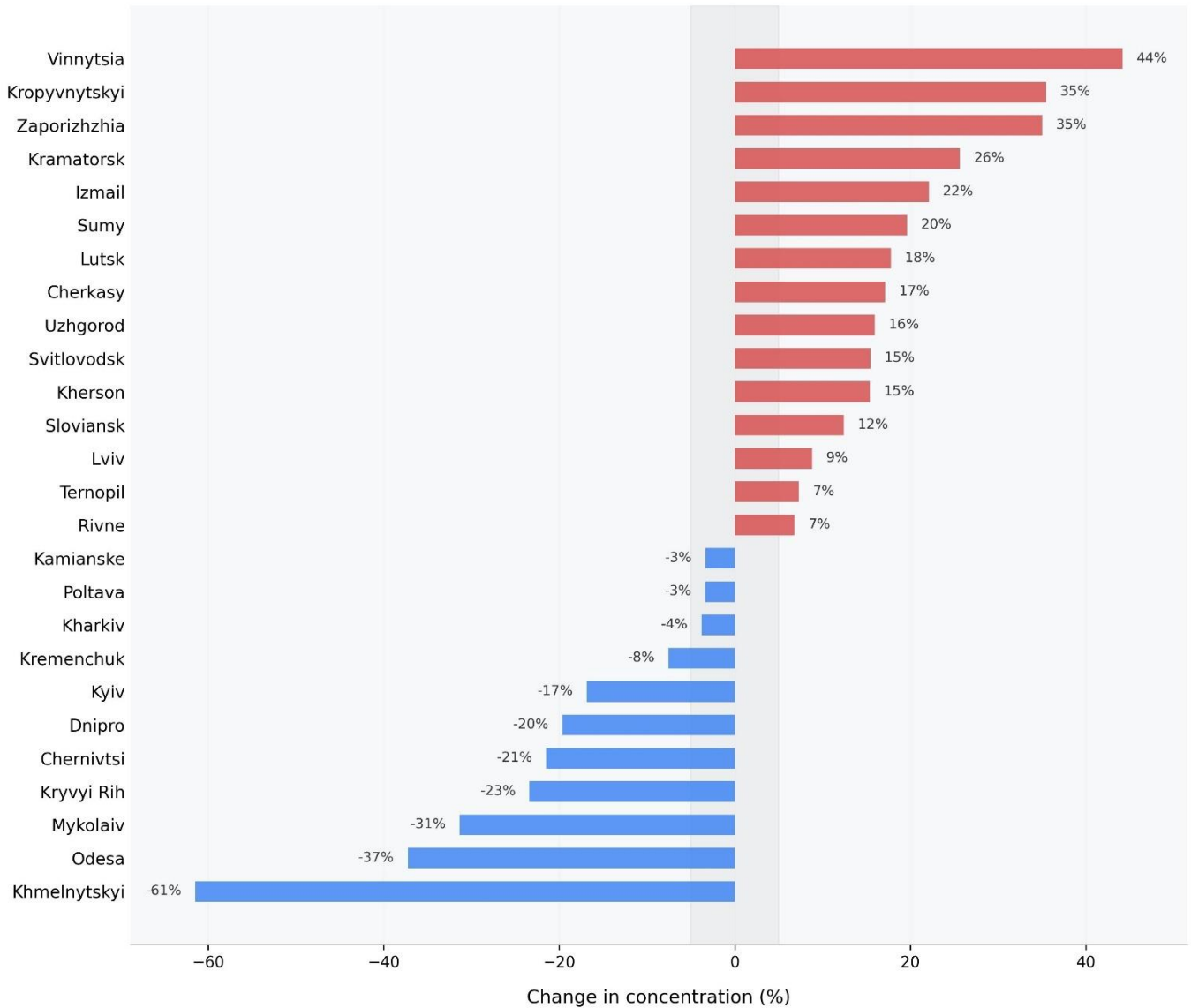


Fig. 16. Percentage change in average concentrations of formaldehyde (CH<sub>2</sub>O) in atmospheric air based on ground-based monitoring data during the period of the full-scale invasion (March 2022 – December 2025), compared with average concentrations for the baseline period (2019–2021) \*

\* Note on result interpretation: the values shown in the plot represent aggregated changes in local pollution within the locations of monitoring stations, which may not correspond to overall patterns for the entire city or its individual districts.

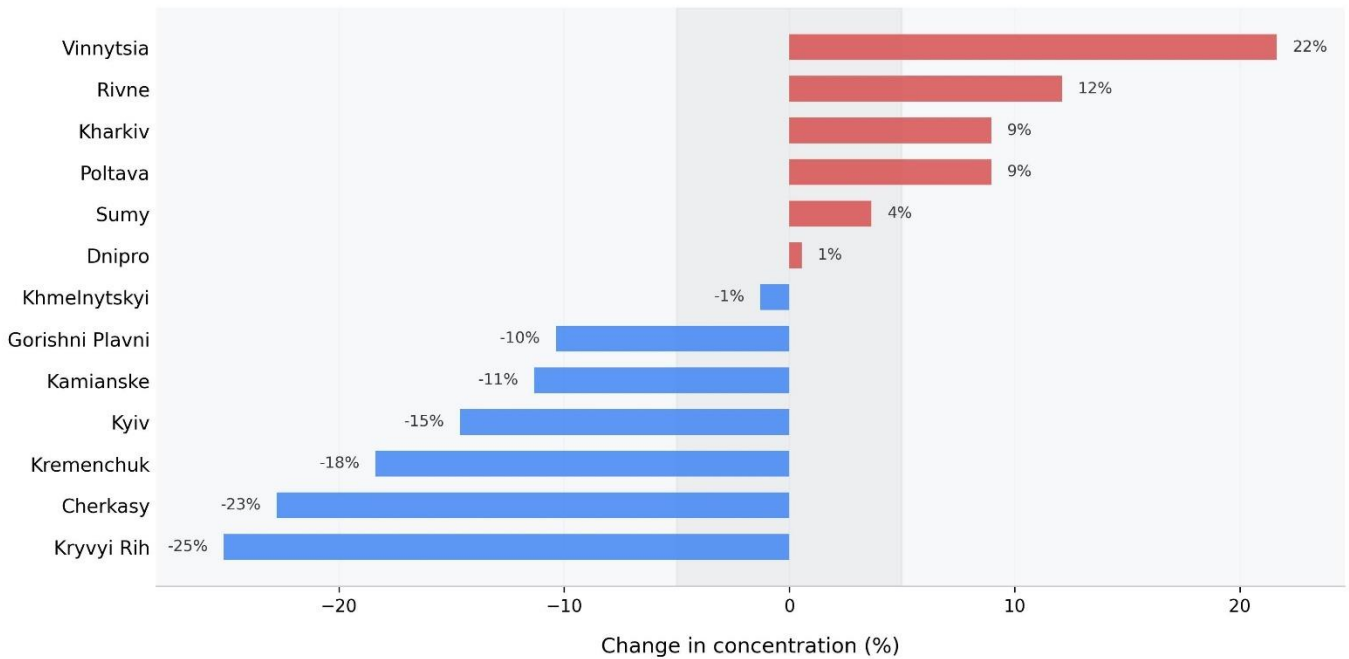
**NH<sub>3</sub>**

Fig. 17. Percentage change in average concentrations of ammonia (NH<sub>3</sub>) in atmospheric air based on ground-based monitoring data during the period of the full-scale invasion (March 2022 – December 2025), compared with average concentrations for the baseline period (2019–2021) \*

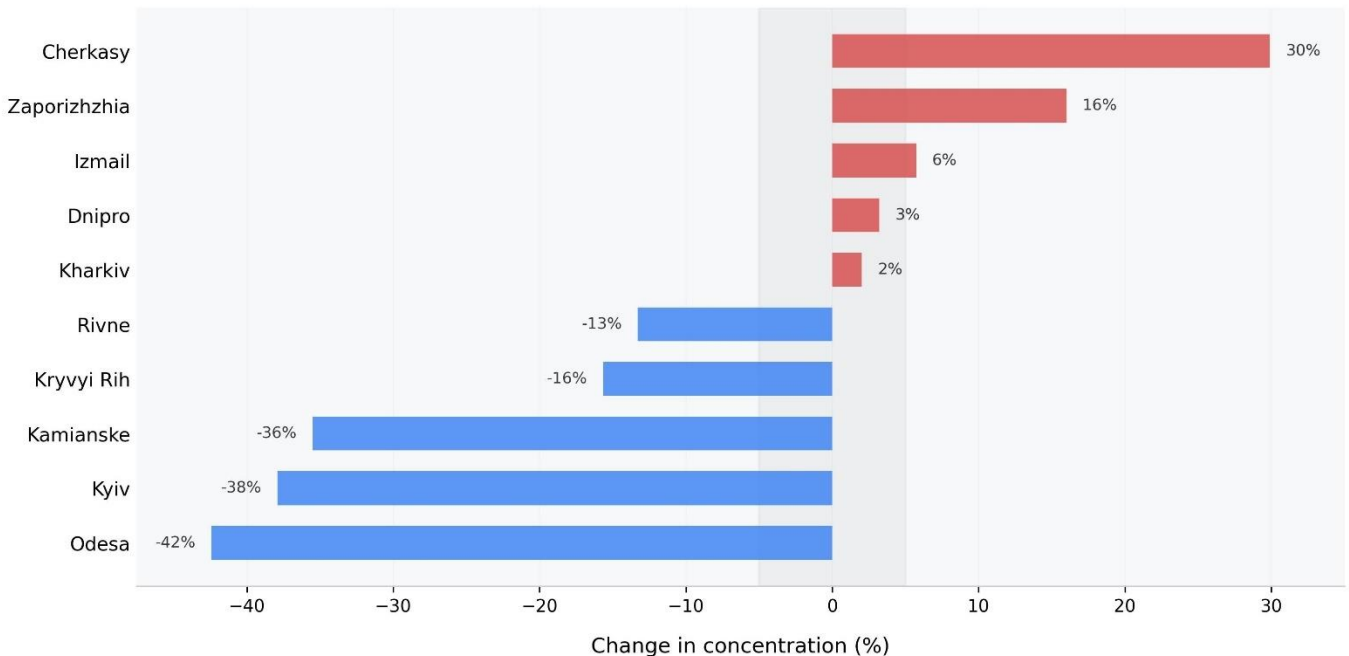
**H<sub>2</sub>S**

Fig. 18. Percentage change in average concentrations of hydrogen sulfide (H<sub>2</sub>S) in atmospheric air based on ground-based monitoring data during the period of the full-scale invasion (March 2022 – December 2025), compared with average concentrations for the baseline period (2019–2021) \*

\* Note on result interpretation: the values shown in the plot represent aggregated changes in local pollution within the locations of monitoring stations, which may not correspond to overall patterns for the entire city or its individual districts.

## HCl

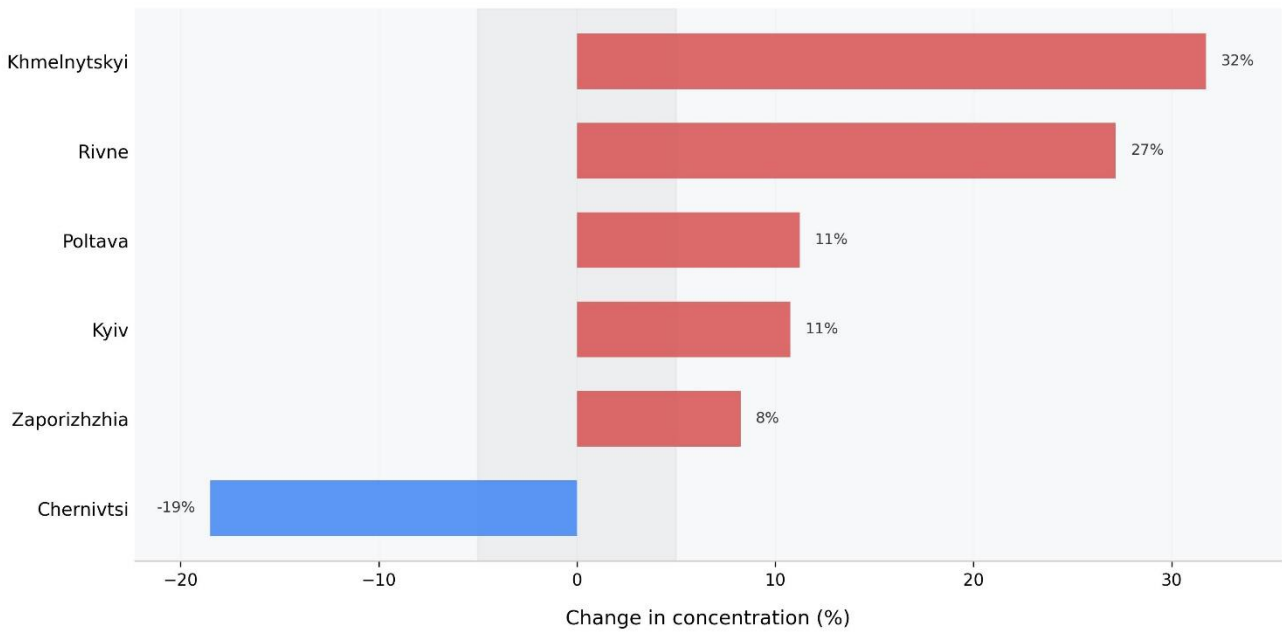


Fig. 19. Percentage change in average concentrations of hydrogen chloride (HCl) in atmospheric air based on ground-based monitoring data during the period of the full-scale invasion (March 2022 – December 2025), compared with average concentrations for the baseline period (2019–2021) \*

## HF

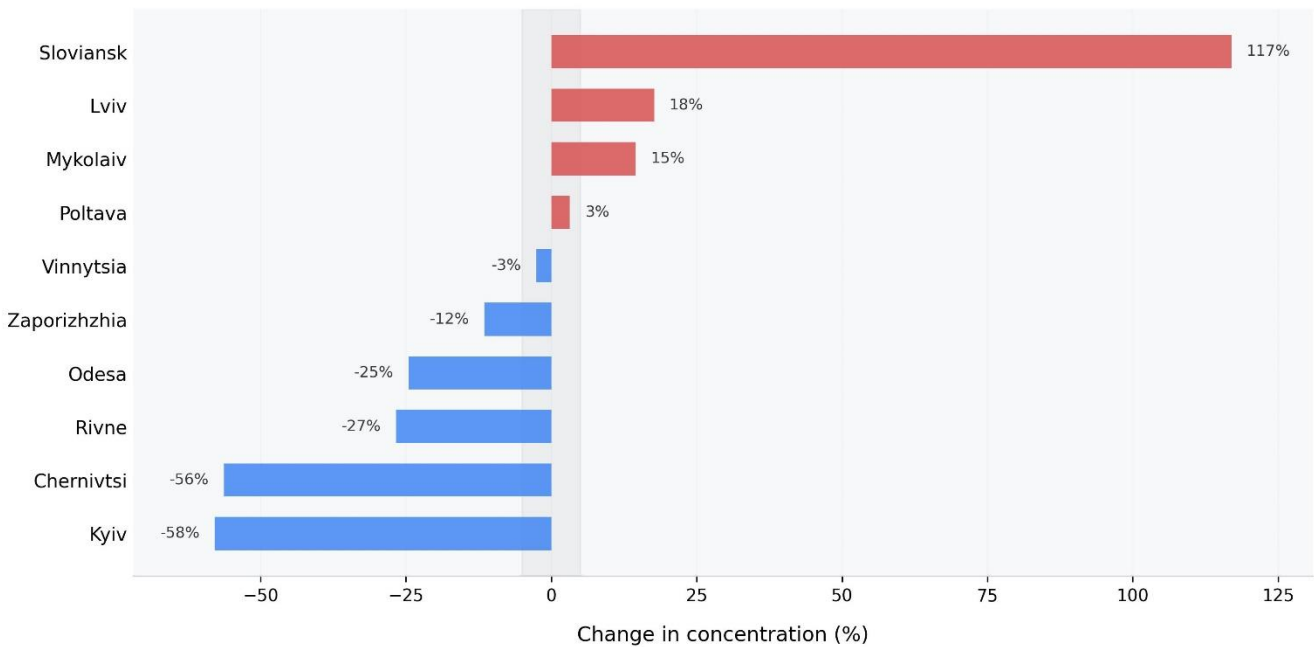


Fig. 20. Percentage change in average concentrations of hydrogen fluoride (HF) in atmospheric air based on ground-based monitoring data during the period of the full-scale invasion (March 2022 – December 2025), compared with average concentrations for the baseline period (2019–2021) \*

\* Note on result interpretation: the values shown in the plot represent aggregated changes in local pollution within the locations of monitoring stations, which may not correspond to overall patterns for the entire city or its individual districts.

The analysis of long-term effects of military actions on air quality based on Sentinel-5P satellite data is limited by the accuracy of retrieving the concentrations of different chemical species. For NO<sub>2</sub>, CO, SO<sub>2</sub>, and CH<sub>2</sub>O, overall changes over four years of the full-scale Russian invasion were analyzed. Due to the high noise levels in satellite data for SO<sub>2</sub> and CH<sub>2</sub>O, these pollutants were excluded from the analysis of seasonal distribution across years.

Assessment of overall air quality based on satellite remote sensing is best performed using NO<sub>2</sub> levels, which is associated with three main factors. First, NO<sub>2</sub> fields are formed by emissions from the vast majority of emission sources<sup>16,17</sup>. Second, satellite retrieval accuracy for NO<sub>2</sub> is higher compared to other gaseous pollutants<sup>18,19</sup>. Third, NO<sub>2</sub> has a relatively short atmospheric lifetime<sup>20</sup>, which leads to localization of concentration maxima around major emission sources and prevents overly smoothed spatial distributions when averaging (as is the case, for example, with CO). [Fig. 21](#) presents seasonal changes in NO<sub>2</sub> VCD in the vertical atmospheric column during the period of the full-scale Russian invasion.

It should be noted that the seasonal NO<sub>2</sub> change maps show localized clusters of intense decreases. These “stable” clusters, which remain spatially consistent from year to year for a given season and are not associated with cities or industrial areas, indicate not the effects of military activity but rather the presence during the baseline period (2019–2021) of episodic strong emission events – most often large-scale landscape fires. In the calculation of NO<sub>2</sub> changes, these appear as localized decreases exceeding 50%. Such clusters should not be included in the overall interpretation when assessing the impact of military actions on air quality.

Immediately after the start of the full-scale Russian invasion, a large-scale redistribution of emission sources occurred. Among the main consequences was a substantial (more than 30%) decrease in NO<sub>2</sub> over Kyiv and several other cities due to the shutdown of industrial activity and population outflow, which led to reduced transport emissions. These changes were particularly pronounced in spring and summer 2022.

In spring 2022, NO<sub>2</sub> increased by 10–15% in areas of active combat and along the emerging front line, which developed from the southern to the northeastern regions of Ukraine.

However, the most significant changes in atmospheric NO<sub>2</sub> occurred over Russian territory to the northeast of the Ukrainian border, where NO<sub>2</sub> increased by more than 50%, associated with intensified military activity related to attacks on Ukraine. Such strong changes are clearly linked to military activity, as there were no reasons for NO<sub>2</sub> increases due to landscape fires or unfavorable meteorological conditions. Similar increases in NO<sub>2</sub> in areas adjacent to Ukraine were recorded regularly and were characterized by particularly strong rises in spring and autumn during 2022–2024, in summer 2023, and in winter seasons of 2022/23, 2023/24, and 2025/26.

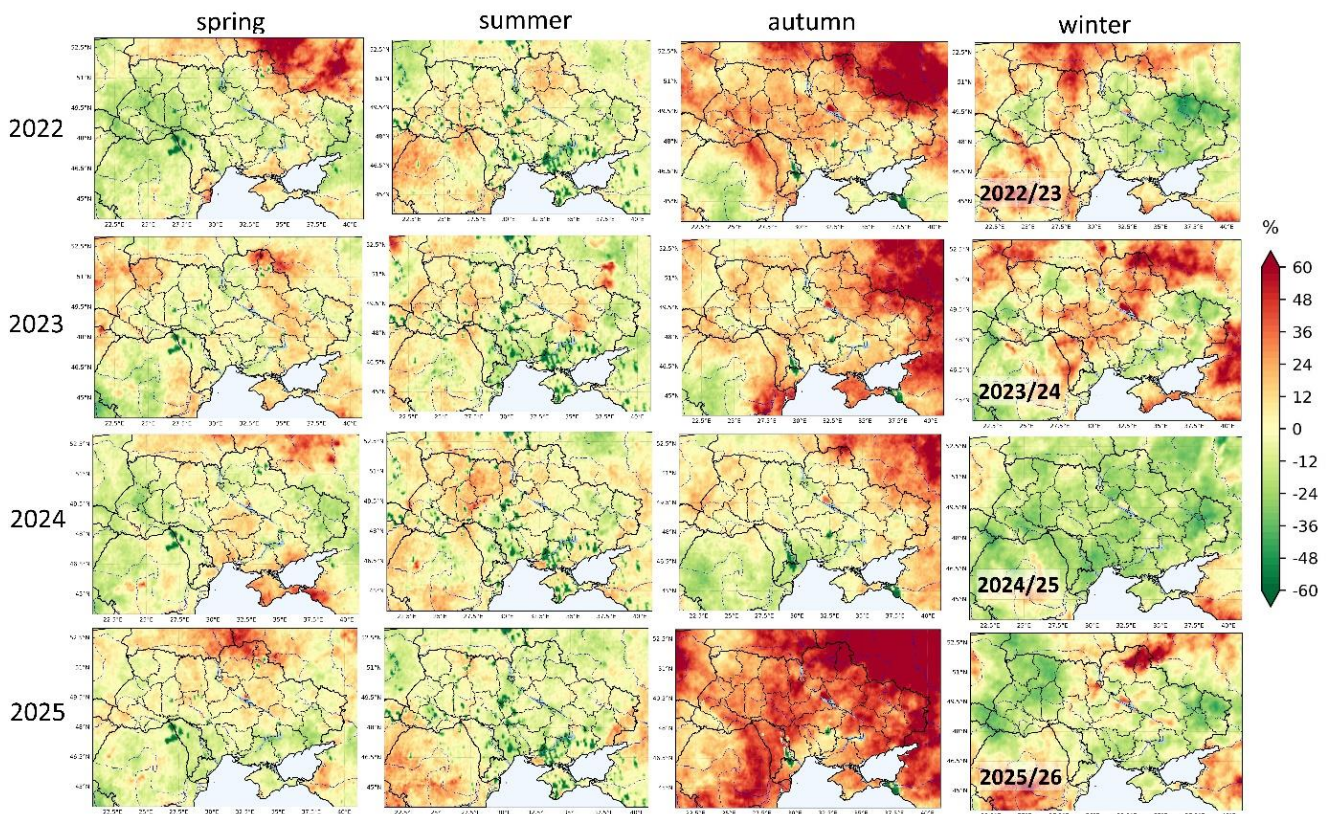


Fig. 21. Percentage change in the seasonal mean tropospheric nitrogen dioxide ( $\text{NO}_2$ ) column density since the beginning of the full-scale invasion (spring 2022 – winter 2025/2026) compared to the mean  $\text{NO}_2$  of the corresponding season during the baseline period (2019–2021)

With the stabilization of the front line, two opposing processes began to be observed along its course: an increase in  $\text{NO}_2$  VCDs due to numerous landscape fires and explosions, and a decrease in  $\text{NO}_2$  due to the destruction of industrial facilities and the complete devastation of cities near the front line. Against the background of continuously alternating increasing and decreasing  $\text{NO}_2$  trends over different periods, the cumulative effect over four years and the scale of economic destruction along the front line outweighed the additional  $\text{NO}_2$  emissions associated with war-related sources.

The influence of meteorological conditions in some cases had a decisive impact on pollution formation. For example, the regional increase in  $\text{NO}_2$  observed in autumn 2025 was a result of lower temperatures and a reduced atmospheric boundary layer height compared to the baseline period, which led to unfavorable conditions for  $\text{NO}_2$  chemical transformation and dispersion.

In contrast to  $\text{NO}_2$ , CO VCDs in the vertical atmospheric column based on Sentinel-5P satellite data do not allow for such a clear identification of long-term changes. Due to the fact that CO has an atmospheric lifetime of several months<sup>21</sup>, emissions are able to spread over large distances, becoming more spatially homogeneous. Even after seasonal averaging, short-term local CO peaks are completely smoothed out, allowing only regional background changes to be identified, which are not related to military activity.

[Fig. 22](#) presents the seasonal changes in total CO content in the vertical atmospheric column during the period of the full-scale Russian invasion.

During the full-scale invasion, CO VCDs showed a regional decrease of 5–20%, particularly in spring and the autumn–winter seasons of 2022 and 2025. An increase in CO was observed mainly during summer seasons, reaching up to 10% relative to the baseline period (2019–2021). Despite the inability of satellite observations to reliably capture war-induced long-term changes in CO, variations in the regional background remain important to consider for correct interpretation, as short-term military-related impacts are superimposed on this background.

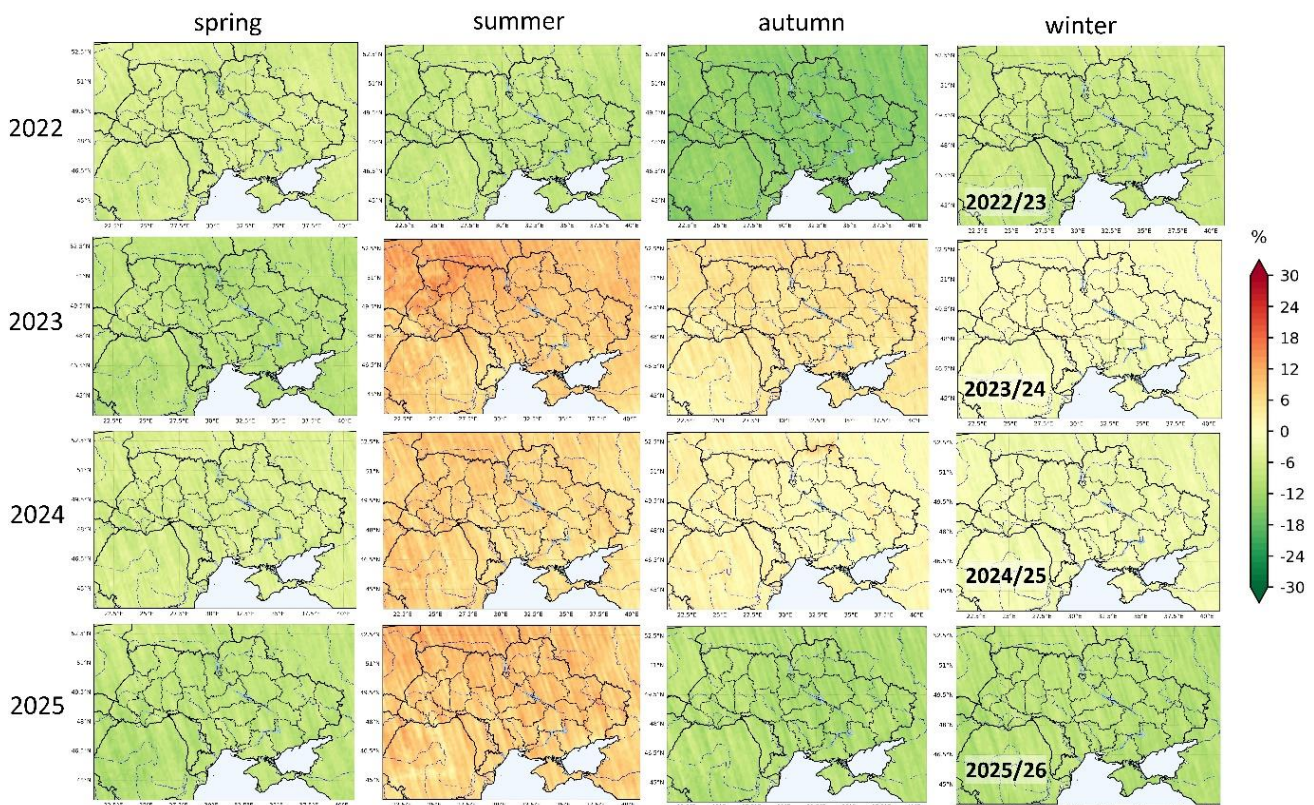


**Fig. 22.** Percentage change in the seasonal mean total carbon monoxide (CO) column density since the beginning of the full-scale invasion (spring 2022 – winter 2025/2026) compared to the mean CO of the corresponding season during the baseline period (2019–2021)

In general, over four years of Russia's full-scale invasion (2022–2026), regional long-term changes in atmospheric pollutant concentrations reflect both war-related impacts and a significant influence of meteorological conditions. [Fig. 23](#) presents the changes in  $\text{NO}_2$ , CO,  $\text{CH}_2\text{O}$ , and  $\text{SO}_2$  VCDs during the period of the full-scale Russian invasion relative to the average content during the baseline period.

The total  $\text{NO}_2$  content primarily reflects the consequences of the large-scale destruction of cities and industrial facilities along the front line, as well as an overall decrease across most regions of Ukraine due to damage and shutdowns of industrial activity. Against this background, localized increases in  $\text{NO}_2$  were recorded mainly in the

Cherkasy, Dnipropetrovsk and Poltava regions. Military activity in Russian territories adjacent to Ukraine, as well as intensified shelling in recent years in the northern parts of the Chernihiv and Sumy regions, led to a marked increase in  $\text{NO}_2$  levels.

The total CO content decreased due to factors not related to military activity, but rather as a result of an overall regional decline and the influence of prevailing meteorological conditions. Mariupol, with the destroyed Azovstal plant, is the only location in Ukraine where long-term CO effects observed in satellite data reflect war-related impacts, in particular a decrease of about 8% against a regional background of 2–3%.

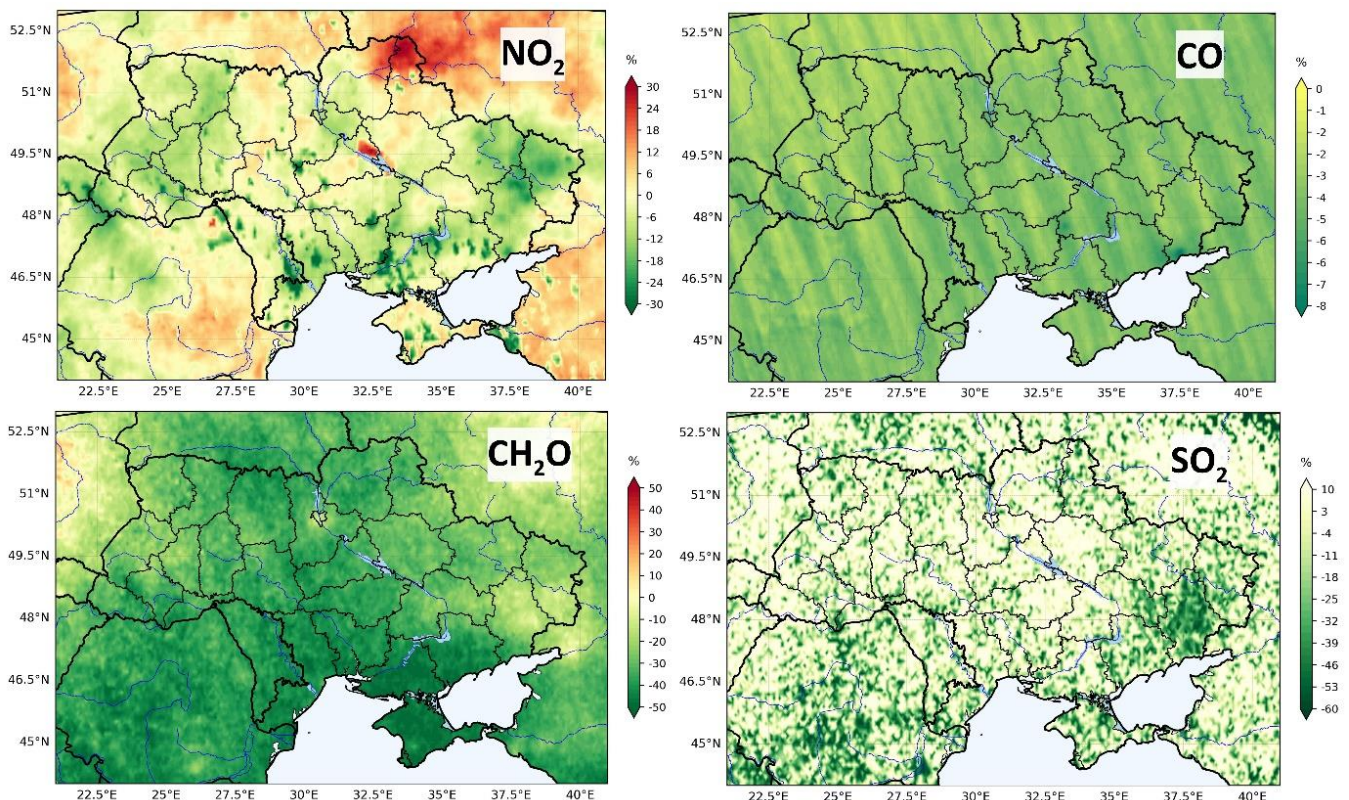


Fig. 23. Percentage change in the tropospheric nitrogen dioxide ( $\text{NO}_2$ ), total carbon monoxide (CO), formaldehyde ( $\text{CH}_2\text{O}$ ) and sulfur dioxide ( $\text{SO}_2$ ) vertical column densities during the full-scale invasion (spring 2022 – winter 2025/2026) compared to the mean vertical column densities during the baseline period (2019–2021)

Satellite data for  $\text{CH}_2\text{O}$  indicate a 10–40% decrease in VCDs due to more favorable prevailing meteorological conditions. The effects of the full-scale Russian invasion on long-term  $\text{CH}_2\text{O}$  trends can be observed only in Kyiv and in cities within the Donetsk and Luhansk regions, where such a decrease was not recorded. However, conclusions based on  $\text{CH}_2\text{O}$  satellite data should be interpreted with caution, as its retrieval sensitivity does not allow for reliable detection of local emission changes and mainly reflects the general state of the atmosphere, including changes in chemical transformation processes occurring above the surface layer. In particular, at the local scale,  $\text{CH}_2\text{O}$  emissions may

increase, which is associated with the widespread use of diesel generators during periods of electricity supply disruptions.

The SO<sub>2</sub> VCDs derived from satellite observations is characterized by a relatively weak signal and a significant contribution of noise in the retrieval process. This results in an extremely spotted spatial distribution of SO<sub>2</sub>. In this case, meaningful conclusions can only be drawn for areas with high SO<sub>2</sub> concentrations either before or after the start of the full-scale invasion. The only region of Ukraine where the signal exceeds the noise component in the analysis of long-term changes is Donetsk Oblast. Across most of this region, SO<sub>2</sub> decreased by 30–50% due to the destruction of energy infrastructure and industrial facilities operating on coal.

As a result, the long-term effects of Russia's full-scale invasion on air quality, based on a combined analysis of ground-based and satellite observations, primarily demonstrate the catastrophic consequences of the destruction of economic capacity. This is visible as a decrease in average pollutant concentrations in industrial cities and, more broadly, at the national scale. At the same time, with increasing proximity to the front line and the border with the Russian Federation, numerous localized hotspots of persistently high surface-level pollution are formed due to emissions from regular shelling of cities. Although these localized hotspots are largely not reflected at the regional scale when analyzing the total pollutant content in the atmospheric column, surface-level trends in average pollutant concentrations often exceed a 50% increase relative to baseline values (i.e., prior to the full-scale invasion).

## CONCLUSIONS

Military activities cause substantial changes in the formation of pollution, associated with an increased frequency of short-term episodes of extremely high concentrations due to missile and drone strikes, the redistribution of pollutant emission sources, disruptions in the regularity of emissions from industrial facilities and road transport, and changes in the characteristics of landscape fires. The manifestation of the impacts of military activities on atmospheric pollution differs at local and regional spatial scales and demonstrates both increasing and decreasing trends in pollutant concentrations depending on the temporal scale of the processes (short-term events and long-term effects). Due to differences in the atmosphere's self-cleaning capacity, accounting for the influence of prevailing meteorological conditions is important for consideration in pollution analysis.

The main consequence of military activities for atmospheric air quality is a sharp, relatively short-term increase in pollutant concentrations caused by emissions released after missile and drone strikes. Due to the limited spatial coverage of ground-based monitoring, only 443 cases of high pollution events during 2022–2025 were identified as consequences of attacks on Ukrainian cities, accounting for less than 1% of all recorded strikes. On average, these events resulted in a 100–300% increase in near-surface concentrations of major pollutants, while increases could exceed 1000% during the most extreme emission events.

Available satellite observations of atmospheric chemical composition helped to somehow expand additional consequences of missile and drone strikes for air quality (primarily for NO<sub>2</sub> and CO). However, the total number of reliable identifications remains extremely low due to limitations associated with cloud cover, insufficient sensor sensitivity to detect increases in pollutant content in the atmospheric column above already polluted urban areas, and the fact that chemical composition data for 2022–2026 are available only from polar-orbiting satellites (i.e., providing a single observation per day). In the case of short-term pollution episodes caused by landscape fires, including those along the front line, satellite data remain the only source of observations that enables quantitative assessment of changes in air quality.

The long-term effects of the Russian full-scale invasion during 2022–2026 primarily reflect the catastrophic consequences of the destruction of industrial facilities and the devastation of cities closer to the front line. At the regional scale, satellite observations revealed a decrease in the VCDs of chemical components. Changes in the background concentrations of pollutants and the influence of prevailing meteorological conditions compared with the 2019–2021 period enhanced the manifestation of these effects. However, even against this background, a decrease in long-term average concentrations

of NO<sub>2</sub> and CO in industrial cities across Ukraine, as well as SO<sub>2</sub> over the territory of Donetsk Oblast, can be identified.

Despite regional trends in pollutant concentration changes, differences in the formation of pollution are more clearly detectable at the local level within the surface layer. Overall, three main long-term effects of military activities on near-surface pollutant concentrations were identified:

1) an increase in atmospheric air pollution in frontline cities, directly associated with active military operations;

2) a decrease in average pollution levels in large industrial cities, primarily due to the destruction of industrial facilities;

3) a redistribution of pollutant concentrations in rear-area cities.

## RECOMMENDATIONS

The main challenge in assessing atmospheric air pollution under wartime conditions is the discrepancy between the need for pollutant concentration data and the actual possibilities of obtaining such data. Unlike peacetime conditions, the number of extreme pollution events requiring additional analysis increases dramatically. Under these circumstances, the need for broader monitoring coverage becomes more critical. However, military activities lead to the opposite situation: infrastructure is lost, monitoring stations are partially destroyed, and observations become impossible as one approaches the front line. Satellite observations help assess overall trends and identify the consequences of individual cases; however, the study of the period of Russia's full-scale invasion clearly demonstrated the critical limitations of existing satellite monitoring of air pollutants. At the same time, these existing challenges indicate that many of these issues can be at least partially addressed.

First of all, despite the point-based nature of observations and the inability to fully cover the territory, **ground-based monitoring remains the key source of information on air quality**, providing evidence-based records of exceedances of regulatory thresholds after missile and drone strikes. Temporal resolution limitations can be overcome through the modernization and deployment of automated monitoring stations. Despite the high cost of installing stationary monitoring stations equipped with automated instruments providing minute-scale temporal resolution, each additional station significantly improves the ability to detect the consequences of missile and drone strikes, as well as reliably identify year-to-year trends in air quality changes.

Given the presence of multiple air quality monitoring stakeholders in Ukraine, the rapid integration of data from different monitoring networks is highly important. Such integration would enable complementary use of information for analysis and research and would partially address limitations in spatial coverage.

It is important to emphasize the role of non-governmental air quality monitoring networks and the expansion of low-cost sensor networks to provide broader spatial coverage. Combined with stationary monitoring stations operated by official monitoring entities, the integration of low-cost sensor networks provides a valuable indicative component that standardized or reference-grade ground-based monitoring networks are unable to capture. Despite methodological inconsistencies between observations, military activities have demonstrated the importance of obtaining any indicative measurement under conditions where other information sources are unavailable. Each available data source has its own level of reliability and representativeness and must be used accordingly; however, together these sources significantly improve understanding of the consequences of extreme wartime events.

Satellite monitoring of atmospheric pollutants, which at the beginning of Russia's full-scale invasion appeared to be a potential solution to overcome the spatial limitations of ground-based observations, could not replace ground monitoring. Nevertheless, it significantly complemented the results and strengthened conclusions regarding the impacts of the war. Among all limitations of satellite-based air quality monitoring, the most significant drawback was the availability of only polar-orbiting satellites. For example, Sentinel-5P, with observations limited to near-noon hours, provided little benefit for detecting the consequences of Russia's large-scale missile and drone attacks, which occurred mainly at night and in the early morning. Under wartime conditions, **geostationary satellite missions could provide the greatest benefit for atmospheric pollution monitoring**, as they continuously observe the same territory and allow tracking the emergence of emissions as well as the subsequent transport and dispersion of pollution plumes.

In 2025, the geostationary satellite Sentinel-4 was launched for monitoring air quality over Europe. Its spatial coverage will allow complete coverage of Ukraine, while hourly data availability will improve the identification of wartime impacts on atmospheric pollution. If military activities continue, Sentinel-4 data may become an important source of information starting from the end of 2026.

As a result of direct monitoring of impacts, ground-based and satellite observations of atmospheric air pollution represent the primary evidence-based source demonstrating deterioration of air quality. In the context of collecting materials for damage and loss assessment, observations will play a leading role. However, available monitoring data from all sources during 2022–2026 will not allow reconstruction of air pollution changes throughout the entire war period because the amount of available data is insufficient. Numerical modeling of atmospheric processes and the **application of chemical transport models are the only possible tools for reconstructing the evolution of air quality throughout the war**. Currently, research focuses only on individual case studies rather than comprehensive modeling. The main challenges in applying models for such tasks include the creation of emission inventories from extraordinary wartime events, the availability of sufficient computational resources, and funding for such studies. At the same time, this can be achieved in the future through proper problem formulation, allocation of time and resources, and continued support for ongoing research using numerical models.

# Research methodology



## Meteorological data and processing

To account for the potential influence of prevailing meteorological conditions on atmospheric air quality, changes in near-surface air temperature, precipitation, wind speed, and atmospheric boundary layer height were analyzed. Meteorological data were obtained from the [ERA5](#) reanalysis dataset (accessed on 09.05.2026), specifically the set of monthly averaged data<sup>22</sup> for the period from March 2019 to February 2026. Since the assessment report presents changes in pollutant concentrations during the full-scale invasion period (2022–2026) relative to the baseline period (2019–2021), the same temporal division was applied to assess changes in prevailing meteorological conditions. Thus, the assessment was performed as the difference in meteorological parameters during the full-scale invasion period compared with the baseline period. For the analysis of individual cases of air quality deterioration following missile and drone strikes in cities, pollutant concentrations were compared with wind fields using ERA5 reanalysis data, specifically the hourly dataset<sup>23</sup>.

Visualization of meteorological data was performed in Python using the matplotlib, cartopy, geopandas libraries, and several other libraries for data processing and preparation.

## Ground-based atmospheric air pollution monitoring data and processing

The analysis of near-surface pollutant concentrations was conducted using ground-based monitoring data from the network of hydrometeorological organizations of the SESU, which are archived and stored at [CGO](#). The data used in this report cover the period from January 2019 to December 2025, with 2019–2021 defined as the baseline period and the period of military activities defined as 24 February 2022 to 31 December 2025. The first months of 2026 were not included due to the considerable time required for data quality control and further verification of the causes of high pollutant concentrations.

Prior to Russia's full-scale invasion, ground-based air quality monitoring within the network of hydrometeorological organizations was conducted in 39 Ukrainian cities at 126 monitoring stations. With the beginning of the full-scale invasion in 2022, monitoring stations in Lysychansk, Mariupol, Rubizhne, and Siverskodonetsk were lost. No analyses or calculations were performed for the lost monitoring stations in these cities. A significant amount of missing data occurred during the occupation of Kherson, as well as in Kramatorsk and Sloviansk due to extremely difficult conditions for conducting observations. Despite this, the available datasets allowed these cities to be included in the analysis. Overall, 35 cities with ground-based observations were included in the study. These cities, including four that were occupied after 2022, are presented on the map in [Fig. 24](#), together with the location of the front line and the liberated territories.

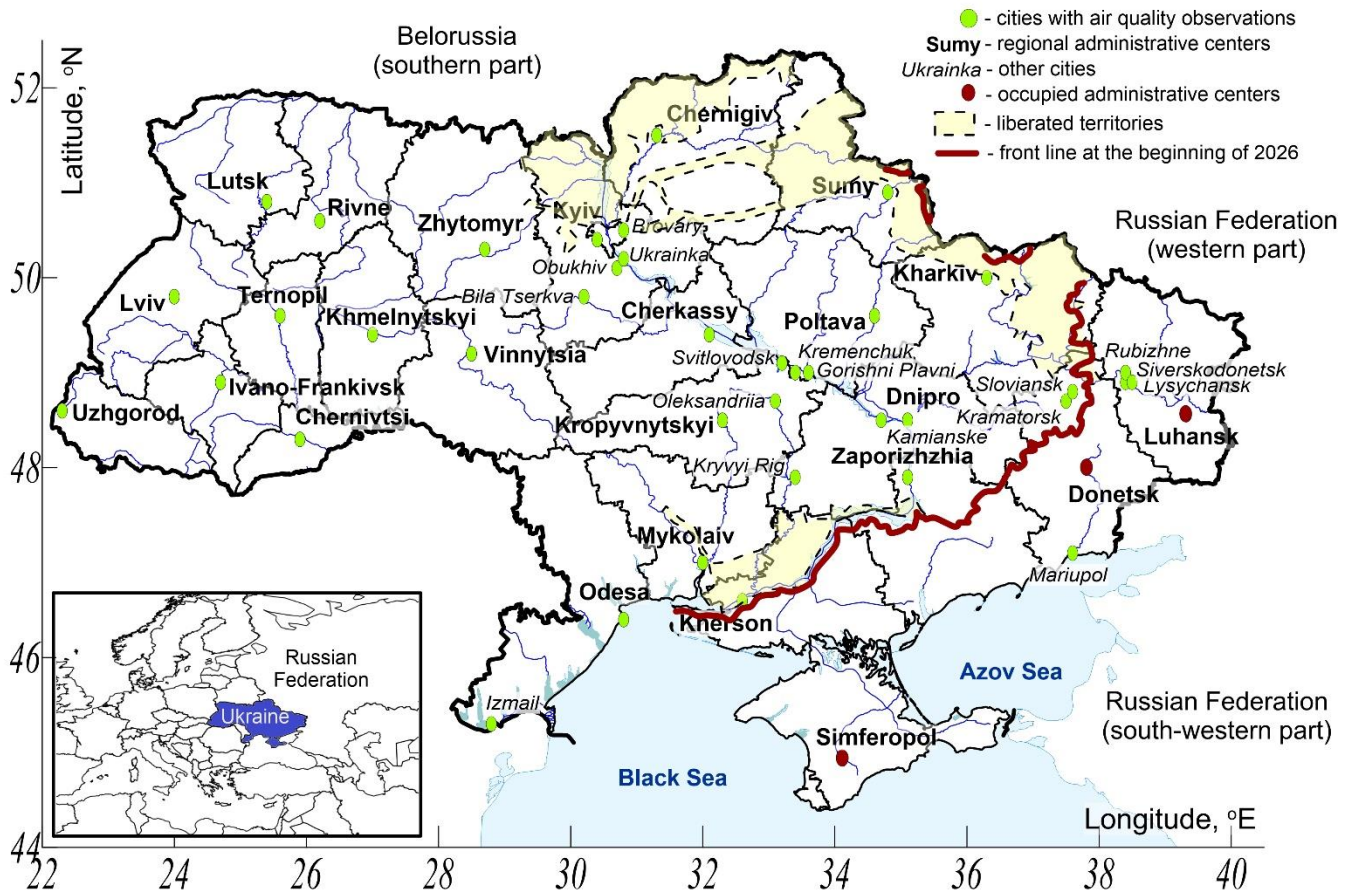


Fig. 24. Map showing the locations of cities with air pollution monitoring stations operated by the network of hydrometeorological organizations of Ukraine

For the analysis, ground-based observation data were used for 11 pollutants: TSP,  $\text{CH}_2\text{O}$ ,  $\text{C}_6\text{H}_5\text{OH}$ , CO,  $\text{H}_2\text{S}$ , HCl, HF,  $\text{NH}_3$ ,  $\text{NO}_2$ , NO, and  $\text{SO}_2$ . A specific feature of the monitoring system operated by the network of hydrometeorological organizations is the availability of only four daily observation times (01:00, 07:00, 13:00, and 19:00), which is related to the outdated state of the instrumentation. Despite these limitations, the hydrometeorological monitoring network provides the most extensive coverage in Ukraine in terms of historical datasets, which is critically important for assessing long-term effects of military activities.

The study of the impacts of Russia's full-scale invasion on near-surface air pollution included the identification of short-term air quality deterioration events following missile and drone strikes, as well as the analysis of long-term effects of the war.

During the analysis of short-term episodes of air quality deterioration in cities, attribution of pollution patterns to missile and drone strikes was performed under the following conditions. First, information about the attack had to be publicly available. Data on missile and drone strikes were collected based on official reports from authorized governmental bodies, as well as using information from the [EcoZagroza](#) platform. Second, a necessary condition was a full temporal and spatial consistency between

increased pollutant concentrations, the timing of the strike, the presence of pollutant emissions, and wind field patterns indicating transport of pollution from the impact site to the monitoring station. Third, the observed increase in pollutant concentrations must not correspond to regular variations in urban pollution (e.g., higher concentrations during rush hours) and must not be influenced by other emission sources with the same transport direction (e.g., during landscape fires). Only under these conditions could an observed concentration increase be conclusively attributed to missile or drone strike impacts.

The analysis of short-term impacts was conducted for pollutants with the best temporal and spatial coverage – CO, NO<sub>2</sub>, SO<sub>2</sub>, and TSP. The increase in concentrations after missile and drone strikes was calculated by comparing pollutant concentrations in the nearest available time interval after the attack with the average concentration during the day preceding the attack.

The analysis of long-term effects was conducted for the full set of 11 selected pollutants by calculating the relative change in average concentration during the period of the full-scale invasion compared with the baseline period.

Processing and visualization of ground-based monitoring data were carried out in Python using the numpy, matplotlib libraries, and several other supporting packages.

## **Satellite observations and data processing**

The study of the VCDs based on satellite remote sensing data was conducted using Sentinel-5P satellite data with the TROPOMI instrument onboard. The original data were downloaded from the official data hub, which as of 2026 is accessible through the [Copernicus Data Space Ecosystem](#) (CDSE, accessed on 08.05.2026).

The dataset used in this report covers the period from February 2019 to February 2026, where 2019–2021 is defined as the baseline period, and the period of military activity is defined as the first four years of Russia's full-scale invasion – from 24 February 2022 to 24 February 2026. Sentinel-5P data are processed daily at UHMI using an automated air quality assessment system<sup>9,24</sup>. More accurate OFFL Level-2 data were selected for the analysis of VCDs for tropospheric NO<sub>2</sub>, CO, SO<sub>2</sub>, and CH<sub>2</sub>O.

The Sentinel-5P OFFL archive at UHMI is archived into daily datasets gridded onto a regular coordinate grid (Level-3 processing) with a horizontal resolution of 0.1°. These data are obtained after filtering the original observations using a qa-value threshold of 0.75 and averaging pixels into predefined 0.1°×0.1° grid cells covering the territory of Ukraine, neighboring countries, and the Black and Azov Sea regions. This gridding approach allows for consistent comparison between adjacent days and enables proper temporal averaging, which is not feasible with raw Level-2 data due to the variable spatial coverage of Sentinel-5P and its 16-day revisit cycle. For the analysis of short-term events,

the same OFFL Level-2 data were used, but in their original horizontal resolution of 3.5×5.5 km at nadir.

The analysis of thermal anomalies for assessing landscape fire distribution was performed using data from Terra (MODIS instrument), Suomi NPP, NOAA-20, and NOAA-21 satellites (VIIRS instrument), obtained from the [Fire Information for Resource Management System](#) (FIRMS, accessed on 09.05.2026). The dataset covers all recorded thermal anomaly events over the territory of Ukraine from March 2019 to February 2026.

Visualization of satellite data was performed in Python using the matplotlib, cartopy, geopandas libraries, and several other tools for data processing and preparation.

## REFERENCES

1. Seinfeld, J.H., & Pandis, S.N. (2016) *Atmospheric Chemistry and Physics: From Air Pollution to Climate Change*. Wiley. ISBN: 978-1-118-94740-1
2. Lazaridis, M. (2011). *First Principles of Meteorology and Air Pollution* (Vol. 19). Springer Netherlands. <https://doi.org/10.1007/978-94-007-0162-5>
3. Cermak, J. E., Davenport, A. G., Plate, E. J., & Viegas, D. X. (Eds.). (1995). *Wind Climate in Cities*. Springer Netherlands. <https://doi.org/10.1007/978-94-017-3686-2>
4. Ueno, H., & Tsunematsu, N. (2019). Sensitivity of ozone production to increasing temperature and reduction of precursors estimated from observation data. *Atmospheric Environment*, 214, 116818. <https://doi.org/10.1016/j.atmosenv.2019.116818>
5. Logan, J. A., Prather, M. J., Wofsy, S. C., & McElroy, M. B. (1981). Tropospheric chemistry: A global perspective. *Journal of Geophysical Research: Oceans*, 86(C8), 7210–7254. <https://doi.org/10.1029/JC086iC08p07210>
6. Sumner, A. L., Shepson, P. B., Couch, T. L., Thornberry, T., Carroll, M. A., Sillman, S., Pippin, M., Bertman, S., Tan, D., Faloon, I., Brune, W., Young, V., Cooper, O., Moody, J., & Stockwell, W. (2001). A study of formaldehyde chemistry above a forest canopy. *Journal of Geophysical Research: Atmospheres*, 106(D20), 24387–24405. <https://doi.org/10.1029/2000JD900761>
7. Savenets M. (2021) Air pollution in Ukraine: a view from the Sentinel-5P satellite. *Idojaras*, 125(2), 271–290. <https://doi.org/10.28974/idojaras.2021.2.6>
8. Pysarenko, L.A. & Savenets, M.V. (2020). Fires in ecosystems and influence on the atmosphere. *Visnyk of V. N. Karazin Kharkiv National University. Series Geology. Geography. Ecology*, 53, 255–266. <https://doi.org/10.26565/2410-7360-2020-53-19> [In Ukrainian]
9. Osadchyi, V., Oreshchenko, A. & Savenets, M. (2023). Satellite monitoring of fires and air pollution. SES of Ukraine, NAS of Ukraine, UHMI. [https://doi.org/10.15407/uhmi.2023\\_1](https://doi.org/10.15407/uhmi.2023_1) [In Ukrainian]
10. Balabukh, V. & Malytska, L. (2017). Impact of climate change on natural fire danger in Ukraine. *Idojaras* 121, 453–477.
11. Savenets, M., Nadtochii, L., Malytska, L., Kozlenko, T., Komisar, K., Umanets, A., Zhemera, N., Hrama, D., & Rudas, M. (2026). Comprehensive analysis of air pollution surface-to-columnar changes after three years of the Russian–Ukrainian war. *Environmental Science and Pollution Research*, 33, 3594–3618. <https://doi.org/10.1007/s11356-026-37512-6>
12. Malytska, L., Galytska, E., Savenets, M., Ladstätter-Weißenmayer, A., & Krajčovičová, J. (2026). The impact of fires on air quality in Ukraine during two years of military conflict (2022–2023): Analyzing satellite, ground-based observations of NO<sub>2</sub>, CO, and aerosols. *Atmospheric Research*, 338, 108959. <https://doi.org/10.1016/j.atmosres.2026.108959>
13. Burning of dry vegetation during martial law in Ukraine may be classified as sabotage! – State Forest Resources Agency of Ukraine. URL: <https://forest.gov.ua/news/spaliuvannia-sukhostoiu-pid-chas-dii-voiennoho-stanu-v-ukraini-mozhe-but-y-pryivniane-do-dyversii> (Accessed: 05.05.2026) [In Ukrainian]
14. Savenets, M., Osadchyi, V., Komisar, K., Zhemera, N., & Oreshchenko, A. (2023). Remotely visible impacts on air quality after a year-round full-scale Russian invasion of Ukraine. *Atmospheric Pollution Research*, 14(11), 101912. <https://doi.org/10.1016/j.apr.2023.101912>
15. Savenets, M. V., Dvoretzka, I. V., Kozlenko, T. V., Komisar, K. M., Umanets, A. P., & Zhemera, N. S. (2023). Status of atmospheric air pollution in Ukraine prior to the full-scale russian invasion. Part 1: ground-level content of pollutants. *Ukrainian Hydrometeorological Journal*, 31, 69-87. <https://doi.org/10.31481/uhmj.31.2023.05> [In Ukrainian]
16. Asilevi, P. J., Dzidzorm, E. N., Boakye, P., & Quansah, E. (2025). Nitrogen dioxide (NO<sub>2</sub>) Meteorology and predictability for air quality management using TROPOMI. *Npj Clean Air*, 1(1), 3. <https://doi.org/10.1038/s44407-024-00003-4>

17. Prunet, P., Lezeaux, O., Camy-Peyret, C., & Thevenon, H. (2020). Analysis of the NO<sub>2</sub> tropospheric product from S5P TROPOMI for monitoring pollution at city scale. *City and Environment Interactions*, 8, 100051. <https://doi.org/10.1016/j.cacint.2020.100051>
18. Tack, F., Merlaud, A., Iordache, M.-D., Pinardi, G., Dimitropoulou, E., Eskes, H., Bomans, B., Veefkind, P., & Van Roozendaal, M. (2021). Assessment of the TROPOMI tropospheric NO<sub>2</sub> product based on airborne APEX observations. *Atmospheric Measurement Techniques*, 14, 615–646. <https://doi.org/10.5194/amt-14-615-2021>
19. Verhoelst, T., Compornolle, S., Pinardi, G., Lambert, J.-C., Eskes, H. J., Eichmann, K.-U., Fjæraa, A. M., Granville, J., Niemeijer, S., Cede, A., Tiefengraber, M., Hendrick, F., Pazmiño, A., Bais, A., Bazureau, A., Boersma, K. F., Bogner, K., Dehn, A., Donner, S., Elokho, A., Gebetsberger, M., Goutail, F., Grutter de la Mora, M., Gruzdev, A., Gratsea, M., Hansen, G. H., Irie, H., Jepsen, N., Kanaya, Y., Karagiozidis, D., Kivi, R., Kreher, K., Levelt, P. F., Liu, C., Müller, M., Navarro Comas, M., Piters, A. J. M., Pommereau, J.-P., Portafaix, T., Prados-Roman, C., Puentedura, O., Querel, R., Remmers, J., Richter, A., Rimmer, J., Rivera Cárdenas, C., Saavedra de Miguel, L., Sinyakov, V. P., Stremme, W., Strong, K., Van Roozendaal, M., Veefkind, J. P., Wagner, T., Wittrock, F., Yela González, M., & Zehner, C. (2021). Ground-based validation of the Copernicus Sentinel-5P TROPOMI NO<sub>2</sub> measurements with the NDACC ZSL-DOAS, MAX-DOAS and Pandonia global networks. *Atmospheric Measurement Techniques*, 14, 481–510. <https://doi.org/10.5194/amt-14-481-2021>
20. Beirle, S., Boersma, K. F., Platt, U., Lawrence, M. G., & Wagner, T. (2011). Megacity Emissions and Lifetimes of Nitrogen Oxides Probed from Space. *Science*, 333(6050), 1737–1739. <https://doi.org/10.1126/science.1207824>
21. Khalil, M. A. K., & Rasmussen, R. A. (1990). The global cycle of carbon monoxide: Trends and mass balance. *Chemosphere*, 20(1–2), 227–242. [https://doi.org/10.1016/0045-6535\(90\)90098-E](https://doi.org/10.1016/0045-6535(90)90098-E)
22. Hersbach, H., Bell, B., Berrisford, P., Biavati, G., Horányi, A., Muñoz Sabater, J., Nicolas, J., Peubey, C., Radu, R., Rozum, I., Schepers, D., Simmons, A., Soci, C., Dee, D., & Thépaut, J.-N. (2023). ERA5 monthly averaged data on single levels from 1940 to present. Copernicus Climate Change Service (C3S) Climate Data Store (CDS). <https://doi.org/10.24381/cds.f17050d7>
23. Hersbach, H., Bell, B., Berrisford, P., Biavati, G., Horányi, A., Muñoz Sabater, J., Nicolas, J., Peubey, C., Radu, R., Rozum, I., Schepers, D., Simmons, A., Soci, C., Dee, D., & Thépaut, J.-N. (2023): ERA5 hourly data on single levels from 1940 to present. Copernicus Climate Change Service (C3S) Climate Data Store (CDS). <https://doi.org/10.24381/cds.adbb2d47>
24. Savenets, M., Oreshchenko, A., & Nadtochii, L. (2022). The system for near-real time air pollution monitoring over cities based on the Sentinel-5P satellite data. *Visnyk of V. N. Karazin Kharkiv National University, Series "Geology. Geography. Ecology"*, 57, 195-205. <https://doi.org/10.26565/2410-7360-2022-57-15>